Nonlinear Dyn (2018) 94:165–184
https://doi.org/10.1007/s11071-018-4351-6

ORIGINAL PAPER

Adaptive dynamic surface neural network control for nonstrict-feedback uncertain nonlinear systems with constraints

Junkang Ni · Ling Liu · Wei He · Chongxin Liu

Received: 16 February 2018 / Accepted: 6 May 2018 / Published online: 17 May 2018
© Springer Science+Business Media B.V., part of Springer Nature 2018

Abstract This paper presents an adaptive dynamic surface neural network control for a class of nonstrict-feedback uncertain nonlinear systems subjected to input saturation, dead zone and output constraint. The problem of input saturation is solved by designing an anti-windup compensator, and the issue of output constraint is addressed by introducing tan-type Barrier Lyapunov function. Furthermore, based on adaptive backstepping technique, a series of novel stabilizing functions are derived. First-order sliding mode differentiator is introduced into backstepping design to obtain the first-order derivative of virtual control. The real control input is obtained using dead-zone inverse method. It is proved that the proposed control scheme can achieve finite time convergence of the output tracking error into a small neighbor of the origin and guarantee all the closed-loop signals are bounded. Simulation results demonstrate the effectiveness of the proposed control scheme.

Keywords Adaptive dynamic surface neural network control · Nonstrict-feedback uncertain nonlinear systems · Input saturation · Dead zone · Output constraint

J. Ni (✉)
The Department of Electrical Engineering, School of Automation, Northwestern Polytechnical University, Xi'an 710072, China
e-mail: max12391@126.com

L. Liu · C. Liu
The State Key Laboratory of Electrical Insulation and Power Equipment, School of Electrical Engineering, Xi'an Jiaotong University, Xi'an 710049, China

W. He
The School of Automation and Electrical Engineering, University of Science and Technology Beijing, Beijing 100083, China

1 Introduction

Recently, the control problem of uncertain nonlinear system has received great attention since many practical systems possess uncertain and nonlinear characteristics. Since many types of neural networks have been proved to have excellent function approximation ability, such as, radial basis function neural network(RBFNN)[1], self-recurrent wavelet neural network [2], recurrent wavelet Elman neural network [3], a series of neural network-based control schemes have been proposed to tackle system uncertainty. In [4], an adaptive neural network tracking control scheme was presented for remotely operated vehicles with unknown dynamic model. In [5], an event-triggered controller using sampled-data neural network was presented for a class of continuous-time nonlinear systems. In [6], an adaptive projection neural network was designed to control redundant manipulators with unknown parameters. In [7], a neural network proportional-derivative control strategy was developed for a teleoperation system. In [8], an adaptive neural network backstepping control method was proposed for nonlower triangular nonlinear systems with unmodeled dynamics. Among these control schemes, adaptive neural network control via backstepping design is particularly attractive and intensive efforts have been devoted to adaptive neural network control via backstepping design. In [9], neural network control was combined with backstepping method to develop a composite controller for a class of strict-feedback uncertain nonlinear systems. In [10], an adaptive neural network control was proposed for uncertain multi-input–multi-output (MIMO) nonlinear systems with block-triangular form. In [11], an observer-based adaptive neural network control was presented for single-input single-output (SISO) stochastic nonlinear systems with unknown time delay. In [12], robust stabilization of nonaffine pure-feedback uncertain nonlinear systems was investigated via adaptive neural network control. In [13], an adaptive neural network backstepping tracking control was designed for an n-link robotic manipulator. In [14], an adaptive backstepping wavelet neural network control was developed for induction motor (IM) drive. In [15], adaptive backstepping-based neural network output feedback control was proposed for uncertain switched stochastic nonlinear systems.

Though adaptive neural network control via backstepping design has become one of the most popular methods to address the control problem of uncertain nonlinear system, an obvious deficiency of traditional backstepping design is the problem of "explosion of complexity" caused by repeated differentiation of virtual control. In particular, when RBFNN is utilized to approximate system uncertainties, we need to take derivative of these radial basis functions, which further increases computation burden. To overcome the "explosion of complexity", adaptive dynamic surface neural network control was presented [16], where first-order filter was introduced to obtain the derivative of virtual control at each step of conventional backstepping. In [17], an adaptive dynamic surface neural network control was developed to achieve fault-tolerant tracking for a class of uncertain nonlinear systems. In [18], dynamic surface control was incorporated into adaptive neural network control to develop a control strategy for a class of uncertain nonlinear systems with pure-feedback form. In [19], an adaptive dynamic surface neural network control with output feedback form was presented for a class of stochastic nonlinear systems. Adaptive dynamic surface neural network control has been applied into many practical systems, such as, underactuated autonomous surface vehicles [20], hypersonic flight vehicles [21–23], flexible joint robots [2], power system [24] and permanent magnet synchronous motor [25]. However, these results fail to consider output constraints and input nonlinearities. In fact, output constraints and input nonlinearities exist in various practical applications.

Output constraint can be found in many practical systems due to physical barrier in the surroundings, safety requirement and system performance specification. If output constraint is ignored in the control design, system performance will be degraded and system damage may occur. Therefore, output constraint plays a very important role in control design. For constrained linear system, reference governor method [26] and convex optimization approach [27] were presented to address output constraint problem. However, these approaches rely on computationally intensive algorithms. To prevent output constraint violation, system transformation techniques were proposed in [28,29] to transform the constrained system into an equivalent unconstrained system. Recently, Barrier Lyapunov function-based design has received great attention since Barrier Lyapunov function tends to infinity when the output approaches some constraints. In [30,31], a logarithm-type Barrier Lyapunov function was presented to handle the issue of output constraint. In [32], a tan-type Barrier Lyapunov function was proposed to avoid output constraint violation. In [33], a cot-type Barrier Lyapunov function was incorporated into Lyapunov function design to deal with constrained state. In [34], an integral Barrier Lyapunov function was designed to prevent the violation of boundary output constraint. In [35,36], an asymmetric time-varying Barrier Lyapunov function was constructed to ensure time-varying output constraint satisfaction. In [37], a time-varying Barrier Lyapunov function was proposed to tackle time-varying output constraint. However, these results fail to consider input nonlinearities. Due to physical constraints in actuator, input nonlinearities can be found in many control systems.

Dead zone and input saturation are common input nonlinearities, which may degrade system performance, reduce control accuracy and even lead to system instability. The existence of dead zone keeps the output of an actuator at zero until the control input exceeds a certain value and the existence of input saturation forces the actuator to give constant output if the control input exceeds a certain value. Therefore, the existence of dead zone and input saturation severely affects the function of control input and makes the control problems complicated and challenging. In order to deal with dead zone, several studies [38–43] modeled the dead zone as a disturbance term and compensated it using disturbance observer or adaptive approach. In [44,45], dead-zone inverse method was adopted to tackle dead-zone problem. In [46,47], neural network and fuzzy logic approximation were employed to compensate the dead zone. To handle the issue of input saturation, some results [48–50] introduced auxiliary system and used its state to develop a constrained control. In [51–53], input saturation was approximated by smooth functions and the approximation error was treated as a disturbance-like term in their control design. In [54], an adaptive scheme was developed to tackle input saturation and achieve output consensus of multiple nonlinear systems subjected to input saturation. In [55], an anti-windup compensator was employed to solve the problem of input saturation. It should be emphasized that the aforementioned control schemes are designed only for the systems that have strict-feedback form or can be transformed into strict-feedback structure, which prohibits broad applications of these methods.

From a mathematical viewpoint, nonstrict-feedback system with the whole system state in each subsystem function is a more general system form. Many practical systems, such as stirred tank reactor process system [56], mass and spring damper system [57], Brusselator [58], electromechanical system [59], have nonstrict-feedback structure. To control nonstrict-feedback system, virtual control should contain the whole system state to deal with the nonlinear function in each subsystem, which will result in algebraic loop problem. This makes the controller design very difficult and challenging. By utilizing monotonous increasing function, variable separation method was developed in [59–62] to design adaptive fuzzy or neural network control for nonstrict-feedback system. However, the above results require that the nonlinear function satisfy the monotonously increasing property. In [63], adaptive neural network tracking problem was considered for nonstrict-feedback switched nonlinear system. In [64], adaptive neural network stabilization problem was investigated for nonlinear system with nonstrict-feedback form. However, these results cannot deal with output constraint and input saturation simultaneously. To the best of our knowledge, there is no studies about nonstrict-feedback nonlinear systems subjected to input saturation, dead zone and output constraint.

Motivated by aforementioned discussion, an adaptive neural network dynamic surface control is proposed for a class of nonstrict-feedback systems subjected to input saturation, dead zone and output constraint. Tan-type Lyapunov function is incorporated into Lyapunov function design to ensure output constraint satisfaction and an anti-windup compensator is introduced to deal with input saturation. Based on backstepping method, a series of novel stabilizing virtual control functions are derived. First-order sliding mode differentiator is presented to obtain the first-order derivative of virtual control and overcome the explosion of complexity problem. Dead-zone inverse approach is adopted to obtain the control input. With the aid of finite time stability theory, the finite time convergence of the output tracking error into a small set around the origin is proved. The main contributions of this paper can be summarized as follows: (1) Based on adaptive neural network dynamic surface control, input saturation, dead zone and output constraint are considered into controller design to address tracking problem for uncertain nonstrict-feedback nonlinear system. To the best of our knowledge, this is the first time to report results about adaptive tracking control for nonstrict-feedback nonlinear system subjected to input saturation, dead zone and output constraint. (2) The proposed control scheme not only overcomes the difficulty of applying backstepping control into nonstrict-feedback system, but also removes the restrictive assumption that the nonlinear function should be monotonous increasing. (3) The finite time tracking problem for uncertain nonstrict-feedback nonlinear system is studied using a series of novel virtual control functions. (4) Different from conventional dynamic surface control, first-order sliding mode differentiator is combined with backstepping design to overcome the explosion of complexity problem, which has finite time convergence property and satisfies separation principle, thereby having superior performance.

2 Preliminary

2.1 Problem formulation

Consider the following uncertain nonlinear system with nonstrict-feedback form:

$$\begin{cases} \dot{x_i} = f_i(x) + g_i(\bar{x}_i)x_{i+1} \\ \dots \\ \dot{x_n} = f_n(x) + g_n(\bar{x}_n)u \\ y = x_1 \end{cases} \tag{1}$$

where $\bar{x}_i = [x_1, \dots, x_i]^{\mathrm{T}}$, $x \in R^n$ denotes state variables. System output $y \in R$ is constrained in open set $|y| < k_c$ with k_c being a positive real number denoting output constraint, $f_i(x)$ and $g_i(\bar{x}_i)$ are unknown smooth nonlinear functions. $u \in R$ is control input subjected to dead zone and input saturation, which can be described as follows:

$$u = \begin{cases} u_{\max} & \text{if } v > v_{\max} \\ m_r(v - b_r) & \text{if } b_r < v \le v_{\max} \\ 0 & \text{if } b_l \le v \le b_r \\ m_l(v - b_l) & \text{if } v_{\min} \le v < b_l \\ u_{\min} & \text{if } v < v_{\min} \end{cases} \tag{2}$$

where v is the desired control input, m_l and m_r are general slopes of dead-zone input, b_l and b_r are left and right breakpoints of dead-zone input, $u_{\max}$ and $u_{\min}$ are the upper and lower bound of $u(t)$. Control input (2) can be rewritten as follows:

$$u = sat(u_d) = \begin{cases} u_{\max}, & \text{if } v > v_{\max} \\ u_d, & \text{if } v_{\min} \le v \le v_{\max} \\ u_{\min}, & \text{if } v < v_{\min} \end{cases}$$

where

$$u_d = K^{\mathrm{T}}(t)\Phi(t)v(t) + \Delta$$
$$K(t) = [K_r(v(t)), K_l(v(t))]^{\mathrm{T}}$$
$$K_r(v(t)) = \begin{cases} m_r, & \text{if } v \ge b_l \\ 0, & \text{else} \end{cases}$$
$$K_l(v(t)) = \begin{cases} m_l, & \text{if } v \le b_r \\ 0, & \text{else} \end{cases}$$
$$\Phi(t) = [\varphi_r(t), \varphi_l(t)]^{\mathrm{T}}$$
$$\varphi_r(t) = \begin{cases} 1, & \text{if } v \ge b_l \\ 0, & \text{else} \end{cases}$$
$$\varphi_l(t) = \begin{cases} 0, & \text{if } v > b_r \\ 1, & \text{else} \end{cases}$$

$$\Delta = \begin{cases} -m_l b_l, & \text{if } v < b_l \\ -(m_l + m_r)v, & \text{if } b_l \le v \le b_r \\ -m_r b_r, & \text{if } v > b_r \end{cases}$$

The error between u and u_d is defined as $\Delta u = u - u_d$.

Remark 1 In system (1), if $f_i(x) = f_i(\bar{x}_i)$ with $\bar{x}_i = [x_1, \dots, x_i]^{\mathrm{T}}$, the system (1) becomes strict-feedback nonlinear system. If $f_i(x) = f_i(\bar{x}_i, 0)$ and $g_i(x) = \partial f_i(\bar{x}_i, x^0_{i+1})/\partial x_{i+1}$ with x^0_{i+1} being a number between 0 and x_{i+1}, the system (1) becomes pure-feedback nonlinear system. Therefore, nonstrict-feedback nonlinear system is a general system form which includes strict-feedback nonlinear system and pure-feedback nonlinear system as its special form [65]. Nonstrict-feedback system can be used to describe many practical systems, such as, stirred tank reactor process system [56], mass and spring damper system [57], Brusselator [58], electromechanical system [59]. Therefore, it is necessary to study control problem for nonstrict-feedback nonlinear system with constraints.

Remark 2 For strict-feedback nonlinear system and pure-feedback nonlinear system, the existing adaptive backstepping control schemes view x_{i+1} as a control input for the first i-th subsystem and a virtual control input α_i is designed to stabilize the first i-th subsystem. To ensure the existence and the uniqueness of the virtual control, α_i should be a function of partial state x_j, $j \le i$. Otherwise, algebraic loop problem will occur. However, the nonlinear function $f_i(x)$ in nonstrict-feedback system contains state x_j, $j > i$. Therefore, the existing adaptive backstepping control schemes for strict-feedback system and pure-feedback system cannot be applied to nonstrict-feedback system. In addition, as shown in [62], it is difficult to tackle the function of x_i descended from previous step to the current design step. Therefore, controlling nonstrict-feedback nonlinear system with constraints is a very difficult and challenging problem.

The studied problem can be formulated as designing an adaptive backstepping control scheme for nonstrict-feedback system (1) such that the system output y can track the reference output y_r within finite time while output constraint is not violated and all the closed-loop signals remain bounded. To this end, the following assumptions are imposed on control parameters, control gain and reference output signal.

Assumption 1 The upper and lower bound of the dead-zone slopes and break points are known: $0 < \underline{m} \leq m_l \leq \bar{m}$, $0 < \underline{m} \leq m_r \leq \bar{m}$, $0 < \underline{b} \leq |b_l| \leq \bar{b}$, $0 < \underline{b} \leq b_r \leq \bar{b}$.

Assumption 2 The signs of $g_i(\bar{x}_i)$ are known and there exist positive constants $\underline{g}_i$ and $\bar{g}_n \geq \underline{g}_n$ such that $\underline{g}_i \leq |g_i(\bar{x}_i)|$ and $\underline{g}_n \leq |g_n(\bar{x}_i)| \leq \bar{g}_n$.

Assumption 3 There exist positive constants B_i such that the reference output signal y_r satisfies $|y_r^{(i)}| \leq B_i$.

Remark 3 According to Assumption 1, there exist positive constants m_0 and $\bar{\Delta}$ such that $K^{\mathrm{T}}(t)\Phi(t) \geq m_0$, $\Delta \leq \bar{\Delta}$.

2.2 Neural network approximation

As we all know, RBFNN can approximate any continuous unknown nonlinear function due to its excellent approximation capability. Here, RBFNN is utilized to approximate a continuous unknown nonlinear function $h(Z)$ as follows:

$$h(Z) = W^{\mathrm{T}} S(Z) \tag{3}$$

where $Z \in \Omega_z \subset R^q$ is RBFNN input vector, $W = [W_1, \ldots, W_l]^{\mathrm{T}} \in R^l$ is RBFNN weight vector, l denotes the number of neurons in hidden layer, $S(Z) = [S_1(Z), \ldots, S_l(Z)]^{\mathrm{T}}$ is radial basis function vector with $S_i(Z) = \exp(-(Z-c_i)^{\mathrm{T}}(Z-c_i)/b_i^2)(i = 1, \ldots, l)$, where $c_i = [c_{i1}, \ldots, c_{iq}]^{\mathrm{T}}$ and b_i represent the center and the width of radial basis function. The ideal weight vector W^* is selected as the value of W that minimizes the approximation error.

$$W^* = \arg \min_{W \in R^l} \left\{ \sup_{Z \in \Omega_Z} |h(Z) - W^{\mathrm{T}} S(Z)| \right\} \tag{4}$$

Using optimal weight vector W^*, the continuous unknown nonlinear function $h(Z)$ can be approximated as follows:

$$h(Z) = W^{*T} S(Z) + \varepsilon \tag{5}$$

where ε is approximation error which is bounded, i.e., $\|\varepsilon\| \leq \bar{\varepsilon}$ with $\bar{\varepsilon}$ being an unknown positive constant.

2.3 Mathematical lemmas

In this section, some useful Lemmas that play an important role in controller design are introduced.

Lemma 1 [66] *For any positive constant γ and any variable $z \in R$, the following inequality holds:*

$$0 \leq |z| - \frac{z^2}{\sqrt{z^2 + \gamma^2}} < \gamma \tag{6}$$

Lemma 2 [67] *For any $a \in R^+$, $b \in R^+$ and $p \in R^+$, $q \in R^+$ satisfying $1/p + 1/q = 1$, the following inequality holds:*

$$ab \leq \frac{a^p}{p} + \frac{b^q}{q} \tag{7}$$

Lemma 3 [68] *For $x_i \in R$ and $0 < b < 1$, we have:*

$$\left(\sum_{i=1}^{n} |x_i| \right)^b \leq \sum_{i=1}^{n} |x_i|^b \tag{8}$$

Lemma 4 [68] *For any real numbers $x_1, \ldots, x_n$ and $0 < p < 1$, one has:*

$$\sum_{i=1}^{n} |x_i|^{1+p} \leq \left(\sum_{i=1}^{n} |x_i|^2 \right)^{(1+p)/2} \tag{9}$$

Lemma 5 [69] *For any positive real numbers α, β and $0 < \gamma < 1$, if a Lyapunov function V satisfies $\dot{V} + \alpha V + \beta V^{\gamma} \leq 0$, then the Lyapunov function V can converge to zero within finite time $T_0 \leq \frac{1}{\alpha(1-\gamma)} \ln \frac{\alpha V^{1-\gamma}(x_0)+\beta}{\beta}$.*

Lemma 6 [70] *For any $\varepsilon > 0$ and $x \in R$, the inequality $|x| - x \tanh(x/\varepsilon) \leq \varrho\varepsilon$ holds, where $\varrho = 0.2785$.*

3 Main results

In this section, a systematic design and stability analysis procedure for the proposed control scheme will be given.

Step 1 Define the error variables as $z_1 = x_1 - y_r$ and the dynamics of the error variables can be expressed as follows:

$$\dot{z}_1 = \dot{x}_1 - \dot{y}_r = g_1(x_1)x_2 + f_1(x) - \dot{y}_r \tag{10}$$

Since the nonlinear function $f_1(x)$ is unknown, RBFNN is used to approximate it.

$$f_1(x) = W_1^{*T} S_1(x) + \varepsilon_1 \tag{11}$$

where $W_1^* = blockdiag[W_{1k}^{*T}](k = 1, \ldots, m)$ is ideal weight vector, $S_1(x)$ is radial basis function vector and ε_1 is approximation error. The approximation error is bounded, i.e., $|\varepsilon_1| \leq \bar{\varepsilon}_1$.

Substituting (11) into (10), one has:

$$\dot{z}_1 = g_1(x_1)x_2 + W_1^{*T} S_1(x) + \varepsilon_1 - \dot{y}_r \tag{12}$$

For notational simplicity, set $M_{z_1} = z_1 / \cos^2(\frac{\pi z_1^2}{2k_b^2})$ and the updating law for neural network weight is designed as follows:

$$\dot{\hat{W}}_1 = \Gamma_1(M_{z_1} S_1(x) - \sigma_1 \hat{W}_1) \tag{13}$$

where Γ_1 and σ_1 are positive real numbers.

The adaptation law for the upper bound of approximation error $\bar{\varepsilon}_1$ is chosen as follows:

$$\dot{\hat{\varepsilon}}_1 = \Lambda_1 \left(\frac{M_{z_1}^2}{\sqrt{M_{z_1}^2 + \gamma_1^2}} - \kappa_1 \hat{\varepsilon}_1 \right) \tag{14}$$

where Λ_1, γ_1 and κ_1 are positive real numbers.

To facilitate virtual control design, define an auxiliary function as follows:

$$\begin{aligned}\bar{\alpha}_1 = {} & k_1 \frac{k_b^2}{\pi} \frac{\sin\left(\frac{\pi z_1^2}{2k_b^2}\right)\cos\left(\frac{\pi z_1^2}{2k_b^2}\right)}{z_1} \\ & + \eta_1 \left(\frac{k_b^2}{\pi}\right)^{\frac{3}{4}} \frac{\cos^2\left(\frac{\pi z_1^2}{2k_b^2}\right) A}{z_1} \\ & + \hat{\varepsilon}_1 \frac{M_{z_1}}{\sqrt{M_{z_1}^2 + \gamma_1^2}} - \dot{y}_r + \hat{W}_1^{\mathrm{T}} S_1(x)\end{aligned} \tag{15}$$

where k_1 and η_1 are positive real numbers and A can be designed as follows:

$$A = \begin{cases} \tan^{3/4}\left(\frac{\pi z_1^2}{2k_b^2}\right), & \text{if } |z_1| \geq \upsilon \\ \tan^{-\frac{1}{4}}\left(\frac{\pi \upsilon^2}{2k_b^2}\right) \tan\left(\frac{\pi z_1^2}{2k_b^2}\right), & \text{else} \end{cases} \tag{16}$$

where $k_b = k_c - B_0$, υ is a positive real number.

With the aid of auxiliary function (15), the virtual control can be designed as follows:

$$\alpha_1 = -\frac{1}{g_1} \frac{M_{z_1} \bar{\alpha}_1^2}{\sqrt{M_{z_1}^2 \bar{\alpha}_1^2 + \gamma_1^2}} \tag{17}$$

Remark 4 The design of (16) is to ensure $\lim_{z_1 \to 0} \frac{\cos^2(\frac{\pi z_1^2}{2k_b^2})A}{z_1} = 0$. In addition, using L'Hospital's rule, we have $\lim_{z_1 \to 0} \frac{1}{z_1} \sin(\frac{\pi z_1^2}{2k_b^2}) \cos(\frac{\pi z_1^2}{2k_b^2}) = 0$. Therefore, (15) does not contain singularity term. Besides, it is worth noting that (16) is continuous, thereby avoiding chattering problem.

From system output constraint and reference output constraint, we have $|z_1| < k_b$ with $k_b + B_0 = k_c$. Select the Barrier Lyapunov function (BLF) as follows:

$$V_b = \frac{k_b^2}{\pi} \tan\left(\frac{\pi z_1^2}{2k_b^2}\right) \tag{18}$$

Remark 5 Tan-type Barrier Lyapunov function has the following properties:

(1) When z_1 approaches k_b, V_b grows to infinity.

(2) $\lim_{k_b \to \infty} \frac{k_b^2}{\pi} \tan(\frac{\pi z_1^2}{2k_b^2}) = \frac{1}{2} z_1^2$

The first property means that tan-type Lyapunov function is a good Barrier Lyapunov function candidate. The second property shows that when there is no constraint, the tan-type Lyapunov function degrades to the commonly used quadratic form. Therefore, tan-type Lyapunov function can deal with both constrained systems and unconstrained systems.

Take BLF (18) into account and the Lyapunov function in the first step can be constructed as follows:

$$V_1 = V_b + \frac{1}{2\Lambda_1} \tilde{\varepsilon}_1^2 + \frac{1}{2\Gamma_1} \tilde{W}_1^{\mathrm{T}} \tilde{W}_1 \tag{19}$$

where $\tilde{\varepsilon}_1 = \bar{\varepsilon}_1 - \hat{\varepsilon}_1$, $\tilde{W}_1 = W_1^* - \hat{W}_1$.

Define the error variable $z_2 = x_2 - \alpha_1$ and the time derivative of V_1 along (12–14) is:

$$\begin{aligned}\dot{V}_1 &= M_{z_1}\dot{z}_1 - \frac{1}{\Lambda_1}\tilde{\varepsilon}_1\dot{\hat{\varepsilon}}_1 - \frac{1}{\Gamma_1}\tilde{W}_1^{\mathrm{T}}\dot{\hat{W}}_1 \\ &= M_{z_1}\left(g_1(x_1)(z_2+\alpha_1) + W_1^{*T}S_1(x) + \varepsilon_1 - \dot{y}_r\right) \\ &\quad - \tilde{\varepsilon}_1\left(\frac{M_{z_1}^2}{\sqrt{M_{z_1}^2+\gamma_1^2}} - \kappa_1\hat{\varepsilon}_1\right) - \tilde{W}_1^{\mathrm{T}}\Big(M_{z_1}S_1(x) \\ &\quad -\sigma_1\hat{W}_1\Big) \\ &= M_{z_1}g_1(x_1)z_2 + M_{z_1}g_1(x_1)\alpha_1 - M_{z_1}\dot{y}_r \\ &\quad + \hat{W}_1^{\mathrm{T}}M_{z_1}S_1(x) + M_{z_1}\varepsilon_1 - \tilde{\varepsilon}_1\frac{M_{z_1}^2}{\sqrt{M_{z_1}^2+\gamma_1^2}} \\ &\quad + \kappa_1\tilde{\varepsilon}_1\hat{\varepsilon}_1 + \sigma_1\tilde{W}_1^{\mathrm{T}}\hat{W}_1\end{aligned} \tag{20}$$

It follows immediately from Lemma 1 that

$$M_{z_1}\varepsilon_1 \le |M_{z_1}|\bar{\varepsilon}_1 < \bar{\varepsilon}_1\gamma_1 + \bar{\varepsilon}_1\frac{M_{z_1}^2}{\sqrt{M_{z_1}^2+\gamma_1^2}} \tag{21}$$

Using Lemma 1 and Assumption 2, we have:

$$M_{z_1}g_1(x_1)\alpha_1 \le -\frac{M_{z_1}^2\bar{\alpha}_1^2}{\sqrt{M_{z_1}^2\bar{\alpha}_1^2+\gamma_1^2}} \le \gamma_1 - M_{z_1}\bar{\alpha}_1 \tag{22}$$

Substituting (15), (17), (21) and (22) into (20) results in

$$\begin{aligned}\dot{V}_1 \le& -k_1\frac{k_b^2}{\pi}\tan\left(\frac{\pi z_1^2}{2k_b^2}\right) - \eta_1\left(\frac{k_b^2}{\pi}\right)^{\frac{3}{4}}\tan^{\frac{3}{4}}\left(\frac{\pi z_1^2}{2k_b^2}\right) + \gamma_1 \\ &+ \bar{\varepsilon}_1\gamma_1 + M_{z_1}g_1(x_1)z_2 + \kappa_1\hat{\varepsilon}_1\tilde{\varepsilon}_1 + \sigma_1\tilde{W}_1^{\mathrm{T}}\hat{W}_1\end{aligned} \tag{23}$$

Step 2 Taking time derivative of error variable z_2 and using RBFNN to approximate unknown nonlinear function $f_2(x)$, we have:

$$\begin{aligned}\dot{z}_2 &= g_2(\bar{x}_2)x_3 + f_2(x) - \dot{\alpha}_1 \\ &= g_2(\bar{x}_2)x_3 + W_2^{*T}S_2(x) + \varepsilon_2 - \dot{\alpha}_1\end{aligned} \tag{24}$$

where $W_2^* = blockdiag[W_{2k}^{*T}](k = 1, \ldots, m)$ is ideal weight vector, $S_2(x)$ is radial basis function vector and ε_2 is approximation error. The approximation error is bounded, i.e., $|\varepsilon_2| \le \bar{\varepsilon}_2$.

In (24), differentiation of virtual control input α_1 leads to the explosion of complexity. In order to overcome the explosion of complexity, first-order sliding mode differentiator is employed to obtain the derivative of the virtual control input.

$$\begin{cases}\dot{\nu}_{11} = -\lambda_0|\nu_{11}-\alpha_1|^{1/2}sign(\nu_{11}-\alpha_1) + \nu_{12} \\ \dot{\nu}_{12} = -\lambda_1 sign(\nu_{11}-\alpha_1)\end{cases} \tag{25}$$

where ν_{11} and ν_{12} are state variables of the differentiator, λ_0 and λ_1 are positive real numbers. According to [71,72], ν_{12} can approximate the first-order derivative of virtual control α_1 to arbitrary accuracy if the initial deviation $|\nu_{11}(t_0) - \alpha_1(t_0)|$ and $|\nu_{12}(t_0) - \dot{\alpha}_1(t_0)|$ are bounded. Therefore, we have $|\nu_{12} - \dot{\alpha}_1| \le \delta_1$ with δ_1 being an unknown positive constant.

Remark 6 Conventional dynamic surface control employs first-order filter to obtain the first-order derivative of virtual control. Different from conventional dynamic surface control, in this paper, first-order sliding mode differentiator is utilized to overcome the explosion of complexity and the poor precision of first-order filter.

The weight updating law for RBFNN is selected as follows:

$$\dot{\hat{W}}_2 = \Gamma_2\left(z_2S_2(x) - \sigma_2\hat{W}_2\right) \tag{26}$$

where Γ_2 and σ_2 are positive real numbers.

The adaptation law for parameters $\bar{\varepsilon}_2$ and δ_1 can be expressed as follows:

$$\dot{\hat{\varepsilon}}_2 = \Lambda_2\left(\frac{z_2^2}{\sqrt{z_2^2+\gamma_2^2}} - \kappa_2\hat{\varepsilon}_2\right) \tag{27}$$

$$\dot{\hat{\delta}}_1 = \Pi_1\left(z_2\tanh(z_2/\varepsilon) - \mu_2\hat{\delta}_1\right) \tag{28}$$

where $\Lambda_2, \Pi_1, \mu_2, \gamma_2$ and κ_2 are positive real numbers.

In order to obtain virtual control, an auxiliary function is designed as follows:

$$\begin{aligned}\bar{\alpha}_2 =& k_2z_2 + \eta_2z_2^{1/2} + \hat{\varepsilon}_2\frac{z_2}{\sqrt{z_2^2+\gamma_2^2}} \\ &- \nu_{12} + \hat{W}_2^{\mathrm{T}}S_2(x) \\ &+ \hat{\delta}_1\tanh(z_2/\varepsilon) + \bar{g}_1\frac{M_{z_1}^2z_2}{\sqrt{M_{z_1}^2z_2^2+\gamma_2^2}}\end{aligned} \tag{29}$$

where k_2 and η_2 are positive real numbers.

Using auxiliary function (29), the virtual control law is derived as follows:

$$\alpha_2 = -\frac{1}{\underline{g}_2}\frac{z_2\bar{\alpha}_2^2}{\sqrt{z_2^2\bar{\alpha}_2^2+\gamma_2^2}} \tag{30}$$

The Lyapunov function can be chosen as follows:

$$V_2 = V_1 + \frac{1}{2}z_2^2 + \frac{1}{2\Lambda_2}\tilde{\varepsilon}_2^2 + \frac{1}{2\Pi_1}\tilde{\delta}_1^2 + \frac{1}{2\Gamma_2}\tilde{W}_2^{\mathrm{T}}\tilde{W}_2 \tag{31}$$

where $\tilde{\varepsilon}_2 = \bar{\varepsilon}_2 - \hat{\varepsilon}_2$, $\tilde{\delta}_1 = \delta_1 - \hat{\delta}_1$, $\tilde{W}_2 = W_2^* - \hat{W}_2$.

Defining $z_3 = x_3 - \alpha_2$ and taking time derivative of V_2 along (24), (26–28), we have:

$$\begin{aligned}
\dot{V}_2 &= \dot{V}_1 + z_2\dot{z}_2 - \frac{1}{\Lambda_2}\tilde{\varepsilon}_2\dot{\hat{\varepsilon}}_2 - \frac{1}{\Pi_1}\tilde{\delta}_1\dot{\hat{\delta}}_1 - \frac{1}{\Gamma_2}\tilde{W}_2^{\mathrm{T}}\dot{\hat{W}}_2\\
&= \dot{V}_1 + z_2\left(g_2(\bar{x}_2)(z_3+\alpha_2)\right.\\
&\quad \left.+ W_2^{*T}S_2(x) + \varepsilon_2 - \dot{\alpha}_1\right)\\
&\quad - \tilde{\delta}_1\left(z_2\tanh(z_2/\varepsilon) - \mu_2\hat{\delta}_1\right)\\
&\quad - \tilde{\varepsilon}_2\left(\frac{z_2^2}{\sqrt{z_2^2+\gamma_2^2}} - \kappa_2\hat{\varepsilon}_2\right)\\
&\quad - \tilde{W}_2^{\mathrm{T}}(z_2S_2(x) - \sigma_2\hat{W}_2)\\
&= \dot{V}_1 + z_2g_2(\bar{x}_2)z_3 + z_2g_2(\bar{x}_2)\alpha_2 + \hat{W}_2^{\mathrm{T}}z_2S_2(x)\\
&\quad + z_2\varepsilon_2 - \tilde{\varepsilon}_2\frac{z_2^2}{\sqrt{z_2^2+\gamma_2^2}} + \kappa_2\tilde{\varepsilon}_2\hat{\varepsilon}_2 - z_2\dot{\alpha}_1\\
&\quad - \tilde{\delta}_1z_2\tanh(z_2/\varepsilon) + \mu_2\tilde{\delta}_1\hat{\delta}_1 + \sigma_2\tilde{W}_2^{\mathrm{T}}\hat{W}_2
\end{aligned} \tag{32}$$

Based on Lemma 1, the following inequality holds:

$$z_2\varepsilon_2 \le |z_2|\bar{\varepsilon}_2 < \bar{\varepsilon}_2\gamma_2 + \bar{\varepsilon}_2\frac{z_2^2}{\sqrt{z_2^2+\gamma_2^2}} \tag{33}$$

From Lemma 1 and Assumption 2, we have:

$$\begin{aligned}
M_{z_1}g_1(x_1)z_2 &\le \bar{g}_1|M_{z_1}||z_2| < \bar{g}_1\gamma_2\\
&\quad + \bar{g}_1\frac{M_{z_1}^2z_2^2}{\sqrt{M_{z_1}^2z_2^2+\gamma_2^2}}
\end{aligned} \tag{34}$$

$$z_2g_2(\bar{x}_2)\alpha_2 \le -\frac{z_2^2\bar{\alpha}_2^2}{\sqrt{z_2^2\bar{\alpha}_2^2+\gamma_2^2}} \le \gamma_2 - z_2\bar{\alpha}_2 \tag{35}$$

Substitute (29), (30) and (33), (35) into (32) and the time derivative of V_2 can be calculated as follows:

$$\begin{aligned}
\dot{V}_2 \le\, &\dot{V}_1 - k_2z_2^2 - \eta_2z_2^{3/2} + z_2\left(\nu_{12} - \dot{\alpha}_1\right)\\
&- z_2\delta_1\tanh(z_2/\varepsilon) + \kappa_2\hat{\varepsilon}_2\tilde{\varepsilon}_2 + \mu_2\hat{\delta}_1\tilde{\delta}_1\\
&+ \sigma_2\tilde{W}_2^{\mathrm{T}}\hat{W}_2 - \bar{g}_1\frac{M_{z_1}^2z_2^2}{\sqrt{M_{z_1}^2z_2^2+\gamma_2^2}}\\
&+ \gamma_2 + z_2g_2(\bar{x}_2)z_3 + \bar{\varepsilon}_2\gamma_2
\end{aligned} \tag{36}$$

Considering $|\nu_{12} - \dot{\alpha}_1| \le \delta_1$ and Lemma 6, we have:

$$\begin{aligned}
&z_2(\nu_{12} - \dot{\alpha}_1) - z_2\delta_1\tanh(z_2/\varepsilon) \le |z_2|\delta_1\\
&\quad - z_2\delta_1\tanh(z_2/\varepsilon)\\
&\quad \le \delta_1\varrho\varepsilon
\end{aligned} \tag{37}$$

Taking (23) together with (34) and (37) into account, (36) becomes:

$$\begin{aligned}
\dot{V}_2 \le &- k_1\frac{k_b^2}{\pi}\tan\left(\frac{\pi z_1^2}{2k_b^2}\right) - \eta_1\left(\frac{k_b^2}{\pi}\right)^{\frac{3}{4}}\tan^{\frac{3}{4}}\left(\frac{\pi z_1^2}{2k_b^2}\right) - k_2z_2^2\\
&- \eta_2z_2^{3/2} + \sum_{i=1}^{2}\left(\kappa_i\hat{\varepsilon}_i\tilde{\varepsilon}_i + \sigma_i\tilde{W}_i^{\mathrm{T}}\hat{W}_i\right) + \mu_2\hat{\delta}_1\tilde{\delta}_1\\
&+ z_2g_2(\bar{x}_2)z_3 + \bar{g}_1\gamma_2 + \sum_{i=1}^{2}(\gamma_i + \bar{\varepsilon}_i\gamma_i) + \delta_1\varrho\varepsilon
\end{aligned} \tag{38}$$

Step i Similar to step 2, the unknown nonlinear function $f_i(x)$ can be approximated using RBFNN and the dynamics of error variables z_i is

$$\begin{aligned}
\dot{z}_i &= g_i(\bar{x}_i)x_{i+1} + f_i(x) - \dot{\alpha}_{i-1}\\
&= g_i(\bar{x}_i)x_{i+1} + W_i^{*T}S_i(x) + \varepsilon_i - \dot{\alpha}_{i-1}
\end{aligned} \tag{39}$$

where $W_i^* = blockdiag[W_{ik}^{*T}](k = 1, \ldots, m)$ is ideal weight vector, $S_i(x)$ is radial basis function vector and ε_i is approximation error. The approximation error is bounded, i.e., $|\varepsilon_i| \le \bar{\varepsilon}_i$.

Similar to step 2, the following first-order sliding mode differentiator is utilized to obtain the derivative of virtual control input:

$$\begin{cases} \dot{\nu}_{(i-1)1} = -\lambda_0|\nu_{(i-1)1} - \alpha_{i-1}|^{1/2} sign(\nu_{(i-1)1} - \alpha_{i-1}) \\ \quad + \nu_{(i-1)2} \\ \dot{\nu}_{(i-1)2} = -\lambda_1 sign(\nu_{(i-1)1} - \alpha_{i-1}) \end{cases} \tag{40}$$

where $\nu_{(i-1)1}$ and $\nu_{(i-1)2}$ are state variables of the differentiator, λ_0 and λ_1 are positive real numbers. According to [71,72], $\nu_{(i-1)2}$ can approximate the first-order derivative of virtual control α_{i-1} to arbitrary accuracy if the initial deviation $|\nu_{(i-1)1}(t_0) - \alpha_{i-1}(t_0)|$ and $|\nu_{(i-1)2}(t_0) - \dot{\alpha}_{i-1}(t_0)|$ are bounded. Therefore, we have $|\nu_{(i-1)2} - \dot{\alpha}_{i-1}| \le \delta_{i-1}$ with δ_{i-1} being an unknown positive constant.

The weight updating law for RBFNN is given as follows:

$$\dot{\hat{W}}_i = \Gamma_i(z_i S_i(x) - \sigma_i \hat{W}_i) \tag{41}$$

where Γ_i and σ_i are positive real numbers.

The adaptive law for parameters $\bar{\varepsilon}_i$ and δ_{i-1} can be described as follows:

$$\dot{\hat{\varepsilon}}_i = \Lambda_i \left(\frac{z_i^2}{\sqrt{z_i^2 + \gamma_i^2}} - \kappa_i \hat{\varepsilon}_i \right) \tag{42}$$

$$\dot{\hat{\delta}}_{i-1} = \Pi_{i-1}\left(z_i \tanh(z_i/\varepsilon) - \mu_i \hat{\delta}_{i-1} \right) \tag{43}$$

where $\Lambda_i, \Pi_{i-1}, \gamma_i, \mu_i$ and κ_i are positive real numbers.

The virtual control can be designed as follows:

$$\alpha_i = -\frac{1}{\underline{g}_i} \frac{z_i \bar{\alpha}_i^2}{\sqrt{z_i^2 \bar{\alpha}_i^2 + \gamma_i^2}} \tag{44}$$

with

$$\begin{aligned} \bar{\alpha}_i &= k_i z_i + \eta_i z_i^{1/2} + \hat{\varepsilon}_i \frac{z_i}{\sqrt{z_i^2 + \gamma_i^2}} - \nu_{(i-1)2} + \hat{W}_i^{\mathrm{T}} S_i(x) \\ &\quad + \hat{\delta}_{i-1} \tanh(z_i/\varepsilon) + \bar{g}_{i-1} \frac{z_{i-1}^2 z_i}{\sqrt{z_{i-1}^2 z_i^2 + \gamma_i^2}} \end{aligned} \tag{45}$$

where k_i, η_i are positive real numbers.

Consider the following Lyapunov function:

$$V_i = V_{i-1} + \frac{1}{2} z_i^2 + \frac{1}{2\Lambda_i} \tilde{\varepsilon}_i^2 + \frac{1}{2\Pi_{i-1}} \tilde{\delta}_{i-1}^2 + \frac{1}{2\Gamma_i} \tilde{W}_i^{\mathrm{T}} \tilde{W}_i \tag{46}$$

where $\tilde{\varepsilon}_i = \bar{\varepsilon}_i - \hat{\varepsilon}_i, \tilde{\delta}_{i-1} = \delta_{i-1} - \hat{\delta}_{i-1}, \tilde{W}_i = W_i^* - \hat{W}_i$.

Define $z_{i+1} = x_{i+1} - \alpha_i$ and the time derivative of V_i along (39), (41–43) is

$$\begin{aligned} \dot{V}_i &= \dot{V}_{i-1} + z_i \dot{z}_i - \frac{1}{\Lambda_i} \tilde{\varepsilon}_i \dot{\hat{\varepsilon}}_i - \frac{1}{\Pi_{i-1}} \tilde{\delta}_{i-1} \dot{\hat{\delta}}_{i-1} \\ &\quad - \frac{1}{\Gamma_i} \tilde{W}_i^{\mathrm{T}} \dot{\hat{W}}_i \\ &= \dot{V}_{i-1} + z_i(g_i(\bar{x}_i)(z_{i+1} + \alpha_i) \\ &\quad + W_i^{*T} S_i(x) + \varepsilon_i - \dot{\alpha}_{i-1}) \\ &\quad - \tilde{\delta}_{i-1}\left(z_i \tanh(z_i/\varepsilon) - \mu_i \hat{\delta}_{i-1} \right) \\ &\quad - \tilde{\varepsilon}_i \left(\frac{z_i^2}{\sqrt{z_i^2 + \gamma_i^2}} - \kappa_i \hat{\varepsilon}_i \right) - \tilde{W}_i^{\mathrm{T}} \left(z_i S_i(x) - \sigma_i \hat{W}_i \right) \\ &= \dot{V}_{i-1} + z_i g_i(\bar{x}_i) z_{i+1} + z_i g_i(\bar{x}_i)\alpha_i + \hat{W}_i^{\mathrm{T}} z_i S_i(x) \\ &\quad + z_i \varepsilon_i - \tilde{\varepsilon}_i \frac{z_i^2}{\sqrt{z_i^2 + \gamma_i^2}} + \kappa_i \tilde{\varepsilon}_i \hat{\varepsilon}_i - z_i \dot{\alpha}_{i-1} \\ &\quad - \tilde{\delta}_{i-1} z_i \tanh(z_i/\varepsilon) + \mu_i \tilde{\delta}_{i-1} \hat{\delta}_{i-1} + \sigma_i \tilde{W}_i^{\mathrm{T}} \hat{W}_i \end{aligned} \tag{47}$$

By Lemma 1, the following inequality is established:

$$z_i \varepsilon_i \le |z_i| \bar{\varepsilon}_i < \bar{\varepsilon}_i \gamma_i + \bar{\varepsilon}_i \frac{z_i^2}{\sqrt{z_i^2 + \gamma_i^2}} \tag{48}$$

According to Lemma 1 and Assumption 2, we have:

$$\begin{aligned} z_{i-1} g_{i-1}(\bar{x}_{i-1}) z_i &\le \bar{g}_{i-1} |z_{i-1}||z_i| \\ &< \bar{g}_{i-1}\gamma_i + \bar{g}_{i-1} \frac{z_{i-1}^2 z_i^2}{\sqrt{z_{i-1}^2 z_i^2 + \gamma_i^2}} \end{aligned} \tag{49}$$

$$z_i g_i(\bar{x}_i)\alpha_i \le -\frac{z_i^2 \bar{\alpha}_i^2}{\sqrt{z_i^2 \bar{\alpha}_i^2 + \gamma_i^2}} \le \gamma_i - z_i \bar{\alpha}_i \tag{50}$$

Substituting (44), (45), (48) and (50) into (47) yields:

$$\begin{aligned} \dot{V}_i \le& \dot{V}_{i-1} - k_i z_i^2 - \eta_i z_i^{3/2} + \kappa_i \hat{\varepsilon}_i \tilde{\varepsilon}_i + \mu_i \hat{\delta}_{i-1} \tilde{\delta}_{i-1} \\ &+ z_i(\nu_{(i-1)2} - \dot{\alpha}_{i-1}) - z_i \delta_{i-1} \tanh(z_i/\varepsilon) \\ &+ \sigma_i \tilde{W}_i^{\mathrm{T}} \hat{W}_i - \bar{g}_{i-1} \frac{z_{i-1}^2 z_i^2}{\sqrt{z_{i-1}^2 z_i^2 + \gamma_i^2}} + \gamma_i \\ &+ z_i g_i(\bar{x}_i) z_{i+1} + \bar{\varepsilon}_i \gamma_i \end{aligned} \tag{51}$$

Similar to step 2, one has:

$$\begin{aligned} & z_i(\nu_{(i-1)2} - \dot{\alpha}_{i-1}) - z_i\delta_{i-1}\tanh(z_i/\varepsilon) \\ & \quad \le |z_i|\delta_{i-1} - z_i\delta_{i-1}\tanh(z_i/\varepsilon) \le \delta_{i-1}\varrho\varepsilon \end{aligned} \tag{52}$$

Substituting (52) and (49) into (51) produces:

$$\begin{aligned} \dot{V}_i \le & -k_1\frac{k_b^2}{\pi}\tan\left(\frac{\pi z_1^2}{2k_b^2}\right) \\ & -\eta_1\left(\frac{k_b^2}{\pi}\right)^{\frac{3}{4}}\tan^{\frac{3}{4}}\left(\frac{\pi z_1^2}{2k_b^2}\right) - \sum_{j=2}^{i}\Big(k_j z_j^2 \\ & +\eta_j z_j^{3/2}\Big) + \sum_{j=1}^{i}\left(\kappa_j\hat{\varepsilon}_j\tilde{\varepsilon}_j + \sigma_j\tilde{W}_j^{\mathrm{T}}\hat{W}_j\right) \\ & + \sum_{j=2}^{i}\left(\mu_j\hat{\delta}_{j-1}\tilde{\delta}_{j-1} + \bar{g}_{j-1}\gamma_j + \delta_{j-1}\varrho\varepsilon\right) \\ & + z_i g_i(\bar{x}_i)z_{i+1} + \sum_{j=1}^{i}\left(\gamma_j + \bar{\varepsilon}_j\gamma_j\right) \end{aligned} \tag{53}$$

Step n In the final design step, the actual control input will be derived. Following the same line used in (24), the dynamics of error variable z_n can be described as follows:

$$\begin{aligned} \dot{z}_n &= g_n(\bar{x}_n)u(v) + f_n(x) - \dot{\alpha}_{n-1} \\ &= g_n(\bar{x}_n)u(v) + W_n^{*T}S_n(x) + \varepsilon_n - \dot{\alpha}_{n-1} \\ &= g_n(\bar{x}_n)(u_d + \Delta u) + W_n^{*T}S_n(x) + \varepsilon_n - \dot{\alpha}_{n-1} \end{aligned} \tag{54}$$

where $W_n^* = blockdiag[W_{nk}^{*T}](k = 1, \ldots, m)$ is ideal weight vector, $S_n(x)$ is radial basis function vector and ε_n is approximation error. The approximation error is bounded, i.e., $|\varepsilon_n| \le \bar{\varepsilon}_n$.

Similar to step 2, the following first-order sliding mode differentiator is utilized to obtain the derivative of virtual control input:

$$\begin{cases} \dot{\nu}_{(n-1)1} = -\lambda_0|\nu_{(n-1)1} - \alpha_{n-1}|^{1/2}sign(\nu_{(n-1)1} \\ -\alpha_{n-1}) + \nu_{(n-1)2} \\ \dot{\nu}_{(n-1)2} = -\lambda_1 sign(\nu_{(n-1)1} - \alpha_{n-1}) \end{cases} \tag{55}$$

where $\nu_{(n-1)1}$ and $\nu_{(n-1)2}$ are state variables of the differentiator, λ_0 and λ_1 are positive real numbers. According to [71,72], $\nu_{(n-1)2}$ can approximate the first-order derivative of virtual control α_{n-1} to arbitrary accuracy if the initial deviation $|\nu_{(n-1)1}(t_0) - \alpha_{n-1}(t_0)|$ and $|\nu_{(n-1)2}(t_0) - \dot{\alpha}_{n-1}(t_0)|$ are bounded. Therefore, we have $|\nu_{(n-1)2} - \dot{\alpha}_{n-1}| \le \delta_{n-1}$ with δ_{n-1} being an unknown positive constant.

By repeating the same way used in step 1, step 2 and step i, we can give the weight updating law for RBFNN, the adaptive law for parameters $\bar{\varepsilon}_n$ and δ_{n-1} as follows:

$$\dot{\hat{W}}_n = \Gamma_n(z_n S_n(x) - \sigma_n\hat{W}_n) \tag{56}$$

$$\dot{\hat{\varepsilon}}_n = \Lambda_n\left(\frac{z_n^2}{\sqrt{z_n^2 + \gamma_n^2}} - \kappa_n\hat{\varepsilon}_n\right) \tag{57}$$

$$\dot{\hat{\delta}}_{n-1} = \Pi_{n-1}\left(z_n\tanh(z_n/\varepsilon) - \mu_n\hat{\delta}_{n-1}\right) \tag{58}$$

where Γ_n, σ_n, γ_n, Λ_n, κ_n, Π_{n-1} and μ_n are positive real numbers.

To deal with input saturation, the following anti-windup compensator is introduced:

$$\dot{w} = \begin{cases} -kw - \xi sig^{1/2}w - \dfrac{\bar{g}_n\frac{z_n^2\Delta u^2}{\sqrt{z_n^2\Delta u^2 + \gamma_n^2}} + \frac{1}{3}(\Delta u)^3}{w} \\ +\Delta u, \quad \text{if } |w| \ge \tau \\ 0, \quad \text{if } |w| < \tau \end{cases} \tag{59}$$

where w is the state of auxiliary design system, k and ξ are positive real numbers to be designed, τ is a small positive constant, $sig^{\alpha}(\cdot) = |\cdot|^{\alpha}sign(\cdot)$.

Remark 7 $|w| < \tau$ means that there is no input saturation and the anti-windup compensator does not work, while $|w| \ge \tau$ means that there exists input saturation and the anti-windup compensator activates to compensate the control input error Δu caused by input saturation.

Considering input saturation and dead zone, the actual control input can be designed as follows:

$$v = -\frac{1}{\underline{g}_n m_0}\frac{z_n\bar{v}^2}{\sqrt{z_n^2\bar{v}^2 + \gamma_n^2}} \tag{60}$$

with

$$\bar{v} = k_n z_n + \eta_n z_n^{1/2} + \hat{\varepsilon}_n \frac{z_n}{\sqrt{z_n^2 + \gamma_n^2}} - \nu_{(n-1)2} + \hat{W}_n^{\mathrm{T}} S_n(x) + \hat{\delta}_{n-1} \tanh(z_n/\varepsilon) + \bar{g}_{n-1} \frac{z_{n-1}^2 z_n}{\sqrt{z_{n-1}^2 z_n^2 + \gamma_n^2}} \tag{61}$$

where k_n, η_n are positive real numbers.

Let us consider the first case where input saturation exists, i.e., $|w| \geq \tau$. Define the following Lyapunov function:

$$V_n = V_{n-1} + \frac{1}{2} z_n^2 + \frac{1}{2\Lambda_n} \tilde{\varepsilon}_n^2 + \frac{1}{2\Pi_{n-1}} \tilde{\delta}_{n-1}^2 + \frac{1}{2} w^2 + \frac{1}{2\Gamma_n} \tilde{W}_n^{\mathrm{T}} \tilde{W}_n \tag{62}$$

where $\tilde{\varepsilon}_n = \bar{\varepsilon}_n - \hat{\varepsilon}_n$, $\tilde{\delta}_{n-1} = \delta_{n-1} - \hat{\delta}_{n-1}$, $\tilde{W}_n = W_n^* - \hat{W}_n$.

Noting that $u_d = K^{\mathrm{T}}(t)\Phi(t)v(t) + \Delta$ and taking time derivative of V_n along (54), (56–59) obtain:

$$\begin{aligned}
\dot{V}_n &= \dot{V}_{n-1} + z_n \dot{z}_n - \frac{1}{\Lambda_n} \tilde{\varepsilon}_n \dot{\hat{\varepsilon}}_n - \frac{1}{\Pi_{n-1}} \tilde{\delta}_{n-1} \dot{\hat{\delta}}_{n-1} + w\dot{w} - \frac{1}{\Gamma_n} \tilde{W}_n^{\mathrm{T}} \dot{\hat{W}}_n \\
&= \dot{V}_{n-1} + z_n (g_n(\bar{x}_n)(u_d + \Delta u) + W_n^{*T} S_n(x) + \varepsilon_n - \dot{\alpha}_{n-1}) \\
&\quad - \tilde{\delta}_{n-1} \left(z_n \tanh(z_n/\varepsilon) - \mu_n \hat{\delta}_{n-1} \right) - \tilde{\varepsilon}_n \left(\frac{z_n^2}{\sqrt{z_n^2 + \gamma_n^2}} - \kappa_n \hat{\varepsilon}_n \right) \\
&\quad - \tilde{W}_n^{\mathrm{T}} \left(z_n S_n(x) - \sigma_n \hat{W}_n \right) \\
&\quad + w(-kw - \xi sig^{1/2} w - \frac{\bar{g}_n \frac{z_n^2 \Delta u^2}{\sqrt{z_n^2 \Delta u^2 + \gamma_n^2}} + \frac{1}{3}(\Delta u)^3}{w} + \Delta u) \\
&= \dot{V}_{n-1} + z_n g_n(\bar{x}_n) \left(K^{\mathrm{T}}(t)\Phi(t)v(t) + \Delta \right) + z_n g_n(\bar{x}_n) \Delta u + \hat{W}_n^{\mathrm{T}} z_n S_n(x) + z_n \varepsilon_n \\
&\quad - \tilde{\varepsilon}_n \frac{z_n^2}{\sqrt{z_n^2 + \gamma_n^2}} - z_n \dot{\alpha}_{n-1} - \tilde{\delta}_{n-1} z_n \tanh(z_n/\varepsilon) \\
&\quad + \kappa_n \tilde{\varepsilon}_n \hat{\varepsilon}_n + \mu_n \tilde{\delta}_{n-1} \hat{\delta}_{n-1} + \sigma_n \tilde{W}_n^{\mathrm{T}} \hat{W}_n - kw^2 \\
&\quad - \xi |w|^{3/2} - \bar{g}_n \frac{z_n^2 \Delta u^2}{\sqrt{z_n^2 \Delta u^2 + \gamma_n^2}} - \frac{1}{3}(\Delta u)^3 + w \Delta u
\end{aligned} \tag{63}$$

Following the same line as step 1, step 2 and step i, we obtain the following inequalities:

$$z_n \varepsilon_n \leq z_n \bar{\varepsilon}_n < \bar{\varepsilon}_n \gamma_n + \bar{\varepsilon}_n \frac{z_n^2}{\sqrt{z_n^2 + \gamma_n^2}} \tag{64}$$

$$z_n g_n(\bar{x}_n) \Delta u \leq \bar{g}_n |z_n||\Delta u| < \bar{g}_n \gamma_n + \bar{g}_n \frac{z_n^2 \Delta u^2}{\sqrt{z_n^2 \Delta u^2 + \gamma_n^2}} \tag{65}$$

$$z_{n-1} g_{n-1}(\bar{x}_{n-1}) z_n \leq \bar{g}_{n-1} |z_{n-1}||z_n| < \bar{g}_{n-1} \gamma_n + \bar{g}_{n-1} \frac{z_{n-1}^2 z_n^2}{\sqrt{z_{n-1}^2 z_n^2 + \gamma_n^2}} \tag{66}$$

$$z_n g_n(\bar{x}_n) K^{\mathrm{T}} \Phi v \leq -\frac{z_n^2 \bar{v}^2}{\sqrt{z_n^2 \bar{v}^2 + \gamma_n^2}} \leq \gamma_n - z_n \bar{v} \tag{67}$$

Invoking Lemma 2, Assumption 2 and Remark 3, we have:

$$w \Delta u \leq \frac{2}{3} |w|^{3/2} + \frac{1}{3} |\Delta u|^3 \tag{68}$$

$$z_n g_n \Delta \leq \bar{g}_n |z_n| \bar{\Delta} \leq \frac{\bar{g}_n}{2} \left(z_n^2 + \bar{\Delta}^2 \right) \tag{69}$$

Substituting (60), (61), (64), (65), (67), (68) and (69) into (63) leads to

$$\begin{aligned}
\dot{V}_n &\leq \dot{V}_{n-1} - \left(k_n - \frac{\bar{g}_n}{2} \right) z_n^2 - \eta_n z_n^{3/2} + z_n \left(\nu_{(n-1)2} - \dot{\alpha}_{n-1} \right) - z_n \delta_{n-1} \tanh(z_n/\varepsilon) \\
&\quad + \gamma_n + \bar{\varepsilon}_n \gamma_n + \bar{g}_n \gamma_n + \kappa_n \tilde{\varepsilon}_n \hat{\varepsilon}_n + \mu_n \tilde{\delta}_{n-1} \hat{\delta}_{n-1} - kw^2 \\
&\quad - \left(\xi - \frac{2}{3} \right) |w|^{3/2} + \sigma_n \tilde{W}_n^{\mathrm{T}} \hat{W}_n + \frac{\bar{g}_n}{2} \bar{\Delta}^2 - \bar{g}_{n-1} \frac{z_{n-1}^2 z_n^2}{\sqrt{z_{n-1}^2 z_n^2 + \gamma_n^2}}
\end{aligned} \tag{70}$$

Similar to step 2 and step i, the following inequality holds:

$$\begin{aligned}
&z_n (\nu_{(n-1)2} - \dot{\alpha}_{n-1}) - z_n \delta_{n-1} \tanh(z_n/\varepsilon) \\
&\leq |z_n| \delta_{n-1} - z_n \delta_{n-1} \tanh(z_n/\varepsilon) \leq \delta_{n-1} \varrho \varepsilon
\end{aligned} \tag{71}$$

Substituting (71) into (70), we have:

$$\dot{V}_n \leq -k_1 \frac{k_b^2}{\pi} \tan\left(\frac{\pi z_1^2}{2k_b^2} \right) - \eta_1 \left(\frac{k_b^2}{\pi} \right)^{\frac{3}{4}} \tan^{\frac{3}{4}} \left(\frac{\pi z_1^2}{2k_b^2} \right)$$

$$
\begin{aligned}
&-\sum_{i=2}^{n-1}\left(k_i z_i^2+\eta_i z_i^{3/2}\right)\\
&-\left(k_n-\frac{\bar{g}_n}{2}\right)z_n^2-\eta_n z_n^{3/2}+\sum_{i=1}^{n}\left(\kappa_i\hat{\varepsilon}_i\tilde{\varepsilon}_i\right.\\
&\left.+\sigma_i\tilde{W}_i^{\mathrm{T}}\hat{W}_i\right)+\sum_{i=2}^{n}\mu_i\hat{\delta}_{i-1}\tilde{\delta}_{i-1}-kw^2\\
&-\left(\xi-\frac{2}{3}\right)|w|^{3/2}\\
&+\sum_{i=2}^{n}(\bar{g}_{i-1}\gamma_i+\delta_{i-1}\varrho\varepsilon)+\bar{g}_n\gamma_n\\
&+\sum_{i=1}^{n}(\gamma_i+\bar{\varepsilon}_i\gamma_i)+\frac{\bar{g}_n}{2}\bar{\Delta}^2
\end{aligned}
\tag{72}
$$

Using Lemma 2, we have:

$$
\begin{aligned}
\tilde{\varepsilon}_i\hat{\varepsilon}_i &\le -\frac{\tilde{\varepsilon}_i^2}{2}+\frac{\varepsilon_i^2}{2}\\
&=-\frac{\tilde{\varepsilon}_i^2}{4}-\frac{1}{4}\left(|\tilde{\varepsilon}_i|-\sqrt{|\tilde{\varepsilon}_i|}\right)^2\\
&\quad+\frac{1}{4}|\tilde{\varepsilon}_i|-\frac{1}{2}|\tilde{\varepsilon}_i|^{3/2}+\frac{\varepsilon_i^2}{2}\\
&\le -\frac{\tilde{\varepsilon}_i^2}{4}+\frac{1}{8}|\tilde{\varepsilon}_i|^2+\frac{1}{8}-\frac{1}{2}|\tilde{\varepsilon}_i|^{3/2}+\frac{\varepsilon_i^2}{2}\\
&\le -\frac{\tilde{\varepsilon}_i^2}{8}+\frac{1}{8}-\frac{1}{2}|\tilde{\varepsilon}_i|^{3/2}+\frac{\varepsilon_i^2}{2}
\end{aligned}
\tag{73}
$$

By repeating the same way used in (73), the following inequalities can be obtained:

$$
\tilde{\delta}_{i-1}\hat{\delta}_{i-1}\le -\frac{\tilde{\delta}_{i-1}^2}{8}+\frac{1}{8}-\frac{1}{2}|\tilde{\delta}_{i-1}|^{3/2}+\frac{\delta_{i-1}^2}{2}
\tag{74}
$$

$$
\tilde{W}_i^{\mathrm{T}}\hat{W}_i\le -\frac{\|\tilde{W}_i\|^2}{8}+\frac{1}{8}-\frac{1}{2}\|\tilde{W}_i\|^{3/2}+\frac{\|W_i\|^2}{2}
\tag{75}
$$

Substituting (73–75) into (72), one has:

$$
\begin{aligned}
\dot{V}_n \le\ & -k_1\frac{k_b^2}{\pi}\tan\left(\frac{\pi z_1^2}{2k_b^2}\right)\\
&-\eta_1\left(\frac{k_b^2}{\pi}\right)^{\frac{3}{4}}\tan^{\frac{3}{4}}\left(\frac{\pi z_1^2}{2k_b^2}\right)-\sum_{i=2}^{n-1}\left(k_i z_i^2\right.\\
&\left.+\eta_i z_i^{3/2}\right)-\left(k_n-\frac{\bar{g}_n}{2}\right)z_n^2\\
&-\eta_n z_n^{3/2}+\sum_{i=1}^{n}\left(-\frac{\kappa_i\tilde{\varepsilon}_i^2}{8}-\frac{\kappa_i}{2}|\tilde{\varepsilon}|^{3/2}-\frac{\sigma_i\|\tilde{W}_i\|^2}{8}\right.\\
&\left.-\frac{\sigma_i}{2}\|\tilde{W}_i\|^{3/2}\right)-\sum_{i=2}^{n}\left(\frac{\mu_i\tilde{\delta}_{i-1}^2}{8}+\frac{\mu_i}{2}|\tilde{\delta}_{i-1}|^{3/2}\right)\\
&-kw^2-\left(\xi-\frac{2}{3}\right)|w|^{3/2}\\
&+\sum_{i=2}^{n}\left(\bar{g}_{i-1}\gamma_i+\frac{\mu_i}{8}+\frac{\mu_i\delta_{i-1}^2}{2}+\delta_{i-1}\varrho\varepsilon\right)+\bar{g}_n\gamma_n\\
&+\sum_{i=1}^{n}\left(\gamma_i+\bar{\varepsilon}_i\gamma_i+\frac{\kappa_i}{8}+\kappa_i\frac{\varepsilon^2}{2}+\frac{\sigma_i}{8}+\frac{\sigma_i\|W_i\|^2}{2}\right)\\
&+\frac{\bar{g}_n}{2}\bar{\Delta}^2
\end{aligned}
\tag{76}
$$

By Lemma 3 and Lemma 4, (76) can be written as follows:

$$
\begin{aligned}
\dot{V}_n \le\ & -k_1\frac{k_b^2}{\pi}\tan\left(\frac{\pi z_1^2}{2k_b^2}\right)-\sum_{i=2}^{n-1}k_i z_i^2-\left(k_n-\frac{\bar{g}_n}{2}\right)z_n^2\\
&-\sum_{i=1}^{n}\frac{\kappa_i\tilde{\varepsilon}_i^2}{8}-\sum_{i=1}^{n}\frac{\sigma_i\|\tilde{W}_i\|^2}{8}-\sum_{i=2}^{n}\frac{\mu_i\tilde{\delta}_{i-1}^2}{8}-kw^2\\
&-\eta_1\left(\frac{k_b^2}{\pi}\right)^{\frac{3}{4}}\tan^{\frac{3}{4}}\left(\frac{\pi z_1^2}{2k_b^2}\right)\\
&-\sum_{i=2}^{n}\eta_i z_i^{3/2}-\sum_{i=1}^{n}\frac{\kappa_i|\tilde{\varepsilon}_i|^{3/2}}{2}\\
&-\sum_{i=1}^{n}\frac{\sigma_i\|\tilde{W}_i\|^{3/2}}{2}-\sum_{i=2}^{n}\frac{\mu_i|\tilde{\delta}_{i-1}|^{3/2}}{2}\\
&-\left(\xi-\frac{2}{3}\right)|w|^{3/2}\\
&+\sum_{i=2}^{n}\left(\bar{g}_{i-1}\gamma_i+\frac{\mu_i}{8}+\frac{\mu_i\delta_{i-1}^2}{2}+\delta_{i-1}\varrho\varepsilon\right)\\
&+\bar{g}_n\gamma_n\\
&+\sum_{i=1}^{n}\left(\gamma_i+\bar{\varepsilon}_i\gamma_i+\frac{\kappa_i}{8}+\kappa_i\frac{\varepsilon^2}{2}+\frac{\sigma_i}{8}+\frac{\sigma_i\|W_i\|^2}{2}\right)\\
&+\frac{\bar{g}_n}{2}\bar{\Delta}^2\\
\le\ & -\beta_1\left(\frac{k_b^2}{\pi}\tan\left(\frac{\pi z_1^2}{2k_b^2}\right)+\frac{1}{2}\sum_{i=2}^{n}z_i^2+\sum_{i=1}^{n}\frac{1}{2\Lambda_i}\tilde{\varepsilon}_i^2\right.\\
&\left.+\sum_{i=1}^{n}\frac{1}{2\Gamma_i}\tilde{W}_i^{\mathrm{T}}\tilde{W}_i+\sum_{i=2}^{n}\frac{1}{2\Pi_{i-1}}\tilde{\delta}_i^2+\frac{1}{2}w^2\right)\\
&-\beta_2\left(\frac{k_b^2}{\pi}\tan\left(\frac{\pi z_1^2}{2k_b^2}\right)+\frac{1}{2}\sum_{i=2}^{n}z_i^2+\sum_{i=1}^{n}\frac{1}{2\Lambda_i}\tilde{\varepsilon}_i^2\right.\\
&+\sum_{i=1}^{n}\frac{1}{2\Gamma_i}\tilde{W}_i^{\mathrm{T}}\tilde{W}_i
\end{aligned}
$$

$$+\sum_{i=2}^{n}\frac{1}{2\Pi_{i-1}}\tilde{\delta}_i^2+\frac{1}{2}w^2\Bigg)^{3/4}+C$$
$$=-\beta_1 V_n-\beta_2 V_n^{3/4}+C \tag{77}$$

where

$$\beta_1=\min\left\{k_1,2k_i,\kappa_i\Lambda_i/4,\sigma_i\Gamma_i/4,\mu_i\Pi_{i-1}/4,2\left(k_n-\frac{\bar{g}_n}{2}\right),\right.$$
$$\left.2k\right\}$$
$$\beta_2=\min\left\{\eta_1,2^{\frac{3}{4}}\eta_i,2^{-\frac{1}{4}}\kappa_i\Lambda_i^{\frac{3}{4}},2^{-\frac{1}{4}}\sigma_i\Gamma_i^{\frac{3}{4}},2^{-\frac{1}{4}}\mu_i\Pi_{i-1}^{\frac{3}{4}},\right.$$
$$\left.2^{\frac{3}{4}}\left(\xi-\frac{2}{3}\right),2^{\frac{3}{4}}\eta_n\right\}$$
$$C=\sum_{i=2}^{n}\left(\bar{g}_{i-1}\gamma_i+\frac{\mu_i}{8}+\frac{\mu_i\delta_{i-1}^2}{2}+\delta_{i-1}\varrho\varepsilon\right)+\bar{g}_n\gamma_n$$
$$+\sum_{i=1}^{n}\left(\gamma_i+\bar{\varepsilon}_i\gamma_i+\frac{\kappa_i}{8}+\kappa_i\frac{\varepsilon^2}{2}+\frac{\sigma_i}{8}+\frac{\sigma_i\|W_i\|^2}{2}\right)$$
$$+\frac{\bar{g}_n}{2}\bar{\Delta}^2$$

If input saturation does not exist, i.e. $|w|<\tau$, the anti-windup compensator does not work and the state of anti-windup compensator keeps zero. In this case, the considered Lyapunov function can be written as follows:

$$V_n=V_{n-1}+\frac{1}{2}z_n^2+\frac{1}{2\Lambda_n}\tilde{\varepsilon}_n^2+\frac{1}{2\Pi_{n-1}}\tilde{\delta}_{n-1}^2+\frac{1}{2\Gamma_n}\tilde{W}_n^{\mathrm{T}}\tilde{W}_n \tag{78}$$

By following the same line as the case where input saturation exists, the time derivative of Lyapunov function (78) can be obtained as follows:

$$\dot{V}_n\le-\beta_1 V_n-\beta_2 V_n^{3/4}+C \tag{79}$$

where

$$\beta_1=\min\left\{k_1,2k_i,\kappa_i\Lambda_i/4,\sigma_i\Gamma_i/4,\mu_i\Pi_{i-1}/4,2\left(k_n-\frac{\bar{g}_n}{2}\right)\right\}$$
$$\beta_2=\min\left\{\eta_1,2^{\frac{3}{4}}\eta_i,2^{-\frac{1}{4}}\kappa_i\Lambda_i^{\frac{3}{4}},2^{-\frac{1}{4}}\sigma_i\Gamma_i^{\frac{3}{4}},2^{-\frac{1}{4}}\mu_i\Pi_{i-1}^{\frac{3}{4}},2^{\frac{3}{4}}\eta_n\right\}$$
$$C=\sum_{i=2}^{n}\left(\bar{g}_{i-1}\gamma_i+\frac{\mu_i}{8}+\frac{\mu_i\delta_{i-1}^2}{2}+\delta_{i-1}\varrho\varepsilon\right)+\sum_{i=1}^{n}\left(\gamma_i+\bar{\varepsilon}_i\gamma_i\right.$$
$$\left.+\frac{\kappa_i}{8}+\kappa_i\frac{\varepsilon^2}{2}+\frac{\sigma_i}{8}+\frac{\sigma_i W_i^2}{2}\right)+\frac{\bar{g}_n}{2}\bar{\Delta}^2$$

The above controller design and stability analysis can be summarized as follows.

Theorem 1 *Consider uncertain nonstrict-feedback nonlinear system (1) with input saturation, dead zone and output constraint. Suppose that Assumptions 1-3 hold. The neural network weight updating law is selected as (13), (26), (41) and (56). The adaptive law for unknown parameters is chosen as (14), (27), (28), (42), (43), (57) and (58). The virtual control laws are designed as (17), (30), (44) and (60). Then, the following properties can be guaranteed: (1) All the closed-loop signals are bounded. (2) The system output constraint will not be violated; (3) System output tracking error will converge to a compact set* $\{z_1:|z_1|<\max\{\upsilon,\sqrt{\tan^{-1}(\frac{C\pi}{\beta_1\varpi k_b^2})\frac{2k_b^2}{\pi}}\}\}$ *within finite time, which can be designed arbitrarily small.*

Proof From (77) and (79), we have:

$$\dot{V}_n<-\beta_1 V_n+C \tag{80}$$

Integrating both side of (80) over $[0,t]$, we obtain:

$$V_n<\left(V_n(0)-\frac{C}{\beta_1}\right)e^{-\beta_1 t}+\frac{C}{\beta_1} \tag{81}$$

The boundedness of Lyapunov function V_n means that Barrier Lyapunov function V_b, the error variables z_i, $\tilde{\varepsilon}_i$, $\tilde{W}_i$, $\tilde{\delta}_i$ and anti-windup state w are bounded. Since $\bar{\varepsilon}_i$ and δ_i are constants, we have that $\hat{\varepsilon}_i$ and $\hat{\delta}_i$ are bounded. Given the fact that z_1 and y_r are bounded, we have that x_1 is bounded. Due to the boundedness of radial basis function $S_i(x)$ and the error variables z_i, from (13), (26), (41) and (56), we have that the neural network weight estimation $\hat{W}_i$ is bounded. From Assumption 3, we have that $\dot{y}_r$ is bounded. Since z_1, $\hat{\varepsilon}_1$, $\dot{y}_r$, $S_1(x)$ and $\hat{W}_1$ are bounded and $\underline{g}_1$ is a constant, from (15) and (17), we can see that $\bar{\alpha}_1$ and α_1 are bounded. Due to the boundedness of z_2 and α_1, we have that x_2 is bounded. Since $\frac{\partial\alpha_1}{\partial\hat{\varepsilon}_1}\dot{\hat{\varepsilon}}_1$, $\frac{\partial\alpha_1}{\partial\dot{y}_r}\ddot{y}_r$, $\frac{\partial\alpha_1}{\partial\hat{W}_1}\dot{\hat{W}}_1$ and $\frac{\partial\alpha_1}{\partial z_1}\dot{z}_1$ are all continuous functions with bounded arguments and δ_1 is a constant, it can be concluded that $\dot{\alpha}_1$ and ν_{12} are bounded. Further, from (25), we have that ν_{11} is bounded. Given the fact that z_1, z_2, $\hat{\varepsilon}_2$, $\hat{\delta}_1$, ν_{12} and $\hat{W}_2$ are bounded and $\bar{g}_1$, $\underline{g}_2$ are constants, we have that $\bar{\alpha}_2$ and α_2 are bounded. Since α_2 and z_3 are bounded, we have that x_3 is bounded. Following the similar analysis procedure, we have that α_i, x_i, ν_{i1}, ν_{i2} and υ are bounded. This follows that the output constraint will not be violated and all the closed-loop signals are bounded.

In order to prove finite time convergence, note that when $C \le \beta_1 \varpi V_n$, we have:

$$\dot{V}_n \le -\beta_1(1-\varpi)V_n - \beta_2 V_n^{3/4} \tag{82}$$

Using Lemma 5, we can deduce that Lyapunov function V_n will converge into a compact set $\{V_n : V_n < \frac{C}{\beta_1 \varpi}\}$ within finite time and the convergence time can be estimated as

$$T \le \frac{4}{\beta_1(1-\varpi)} \ln \frac{\beta_1(1-\varpi)V_n(0)^{1/4} + \beta_2}{\beta_2} \tag{83}$$

If V_n converges to the set $\{V_n : V_n < \frac{C}{\beta_1 \varpi}\}$, we have $\frac{k_b^2}{\pi}\tan(\frac{\pi z_1^2}{2k_b^2}) \le V_n < \frac{C}{\beta_1 \varpi}$, which means that the output tracking error will converge to a compact set $\{z_1 : |z_1| < \max\{\upsilon, \sqrt{\tan^{-1}(\frac{C\pi}{\beta_1 \varpi k_b^2})\frac{2k_b^2}{\pi}}\}$ within finite time T. □

Remark 8 In stability analysis, we only consider the case where $|z_1| \ge \upsilon$ holds in (16) and Theorem 1 shows that the ultimate bound of tracking error z_1 is determined by $\max\{\upsilon, \sqrt{\tan^{-1}(\frac{C\pi}{\beta_1 \varpi k_b^2})\frac{2k_b^2}{\pi}}\}$. If υ is selected sufficiently small such that $\upsilon \le \sqrt{\tan^{-1}(\frac{C\pi}{\beta_1 \varpi k_b^2})\frac{2k_b^2}{\pi}}$, the ultimate bound of z_1 is independent of υ.

Remark 9 Theorem 1 provides a guideline for the designer to select appropriate design parameters such that the ultimate bound of tracking error can be reduced. The ultimate bound of tracking error can be made as small as possible if we choose small C and large β_1. To ensure C as small as possible and β_1 as large as possible, we needs to select small γ_i and large k_i, Λ_i, Γ_i, Π_{i-1}, k.

Remark 10 The approach presented in this paper is partly motivated by the work in [32]. However, the results in [32] can only be used for strict-feedback system with output constraint. In this paper, we address tracking problem for nonstrict-feedback system with input saturation, dead zone and output constraint. To the best of our knowledge, this is the first time to report results about adaptive tracking control for nonstrict-feedback nonlinear system subjected to input saturation, dead zone and output constraint. In addition, the results in [32] are based on backstepping technique which has the problem of explosion of complexity. In this paper, first-order sliding mode differentiator is employed to obtain the first derivative of virtual control, which overcomes explosion of complexity.

4 Comparison with existing results

To highlight the novelty of the obtained results, we make a comparison with the existing results in this section.

(1) The previous studies [9,11,12,16–19,29,31–33,35–38,44–46,48–50,52–54] present adaptive backstepping neural network control schemes for strict-feedback system or pure-feedback system. However, these results cannot be extended to nonstrict-feedback system. As shown in Remark 2, it is very difficult and challenging to apply backstepping design into nonstrict-feedback system. This paper overcomes the difficulty of applying backstepping control into nonstrict-feedback system and proposes a novel adaptive dynamic surface neural network control scheme for nonstrict-feedback system. Since nonstrict-feedback system includes strict-feedback system and pure-feedback system as its special form, the results obtained in this paper are more general and can be applied to address adaptive neural network control problem for strict-feedback system or pure-feedback system.

(2) The previous studies [59–62] employ variable separation technique to overcome the design difficulty arising from nonstrict-feedback structure. However, these results require that the nonlinear function $f_i(x)$ in system (1) satisfies the monotonously increasing property. The results obtained in this paper remove this restrictive assumption and can be applied into more general nonstrict-feedback system.

(3) The previous studies [56–63] can only achieve asymptotical tracking for uncertain nonstrict-feedback nonlinear system. The results obtained in this paper achieve finite time tracking for uncertain nonstrict-feedback nonlinear system.

(4) The previous studies [57–63] present adaptive backstepping neural network control for uncertain nonstrict-feedback nonlinear system. However,

these results suffer from the problem of "explosion of complexity". In order to overcome the "explosion of complexity', adaptive dynamic surface neural network control was developed in [56]. However, it employs command filter to obtain the derivative of virtual control, which has asymptotical convergence property. Different from previous work, in this paper, first-order sliding mode differentiator is combined with backstepping design to overcome the explosion of complexity problem, which has finite time convergence property and satisfies separation principle, thereby having superior performance.

(5) To the best of our knowledge, there are no results about adaptive tracking control for nonstrict-feedback nonlinear system subjected to input saturation, dead zone and output constraint. This paper proposes an adaptive neural network dynamic surface control to address this problem.

5 Simulation results

In this section, two examples are carried out to demonstrate the effectiveness of the proposed control scheme.

Example 1 Consider the following second-order nonstrict-feedback nonlinear system:

$$\begin{cases} \dot{x_1} = f_1(x) + g_1(x_1)x_2 \\ \dot{x_2} = f_2(x) + g_2(\bar{x}_2)u \\ y = x_1 \end{cases} \tag{84}$$

where $f_1(x) = x_1x_2 + x_1^2\sin(x_2)$, $g_1(x_1) = 1.5 + 0.5\sin(x_1)$, $f_2(x) = x_1x_2e^{x_2}$, $g_2(\bar{x}_2) = 1.5 + \sin(x_1x_2)$. Here, it is assumed that $f_1(x)$, $g_1(x_1)$, $f_2(x)$ and $g_2(\bar{x}_2)$ are unknown. Reference output is given as $y_r = \sin(t)$ and the output constraint is selected as $|y| < \pi/2$. It can be easily verified that there exist $\underline{g}_1 = 1, \bar{g}_1 = 2, \underline{g}_2 = 0.5, \bar{g}_2 = 2.5$ such that Assumption 2 holds. Dead zone and input saturation parameters are taken to be $m_r = 1$, $b_r = 0.1$, $m_l = 1.05$, $b_l = -0.15$, $u_{\max} = 5$, $u_{\min} = -4$. The design parameters in virtual control, parameter adaptive law and first-order sliding mode differentiator are chosen as $k_1 = k_2 = 3$, $\eta_1 = \eta_2 = 2.5$, $\Lambda_1 = \Lambda_2 = 2$, $\kappa_1 = \kappa_2 = 5$, $\Gamma_1 = \Gamma_2 = 0.4$, $\sigma_1 = \sigma_2 = 10$, $\Pi_1 = 10$, $\mu_2 = 4.12$, $k = 10$, $\xi = 5$, $\tau = 0.1$, $\gamma_1 = \gamma_2 = 0.1$, $\lambda_0 = 1.5$, $\lambda_1 = 1.1$. The results are

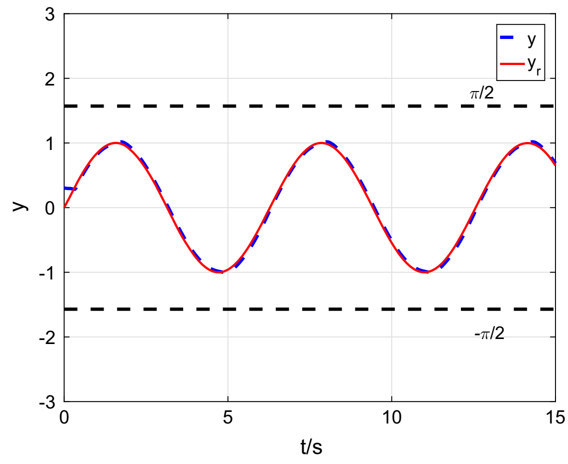

Fig. 1 Time response of system output y and its reference y_r

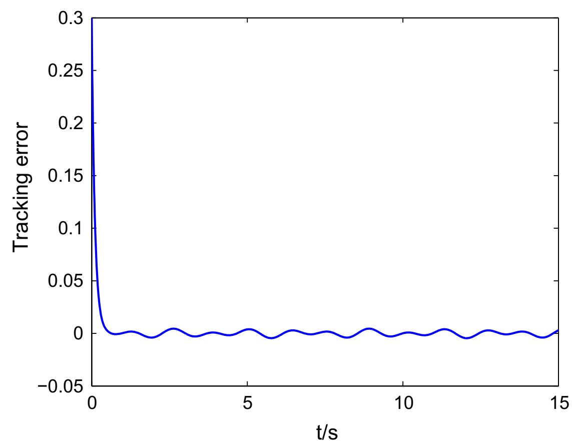

Fig. 2 Time response of tracking error

shown in Figs. 1, 2, 3, 4, 5 and 6. As shown in Fig. 1 that the system output follows the trajectory of reference signal closely without violation of output constraint. As shown in Fig. 2, the tracking error reaches a small neighbor of the origin within finite time and remains in it thereafter. Figure 3 shows the curve of control input u. The estimations of parameters $\bar{\varepsilon}_i$ and δ and the time response of anti-windup compensator state w are depicted in Figs. 4, 5 and 6. It is clear that all the parameter estimations and the anti-windup compensator state are bounded. All the results show that the proposed control scheme can guarantee all the closed-loop signals are bounded and tracking error converges to a small neighbor of the origin within finite time,

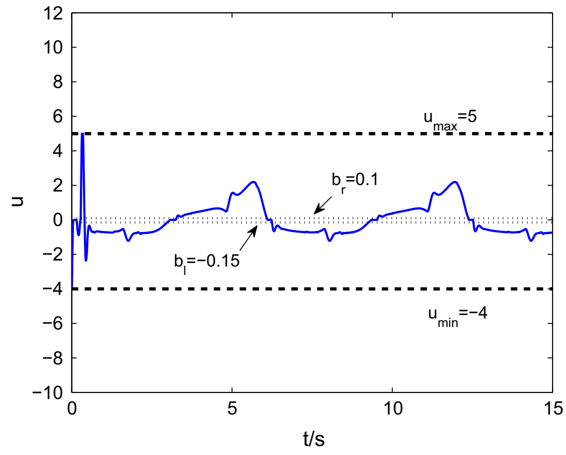

Fig. 3 Curve of control input u

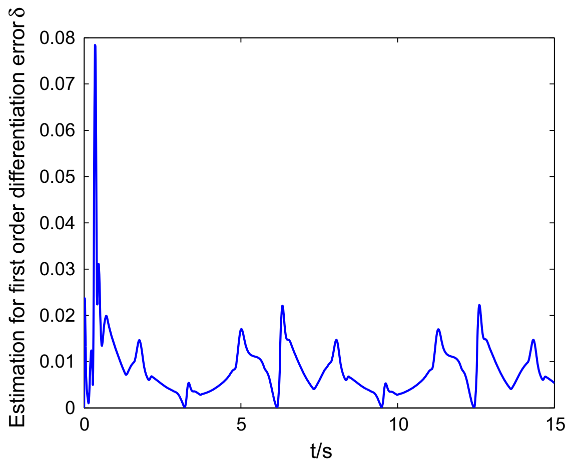

Fig. 5 Time response of estimation error for first-order differentiation error δ

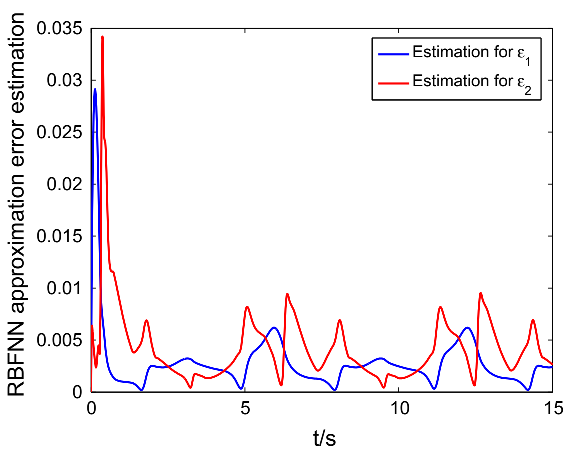

Fig. 4 Time response of RBFNN approximation error estimation $\bar{\varepsilon}_i$

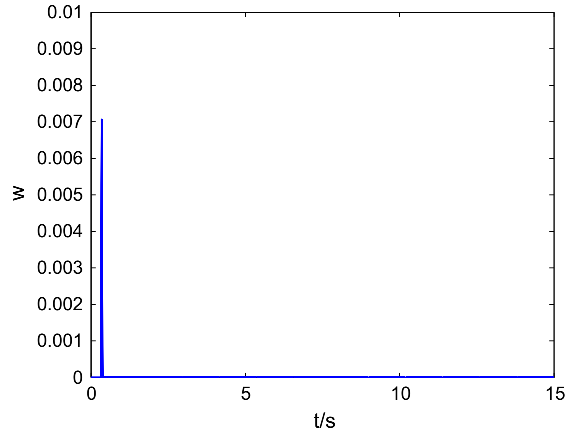

Fig. 6 Time response of anti-windup compensator state w

which verifies the effectiveness of the proposed control scheme.

Example 2 Consider the following system which describes the dynamics of a one-link manipulator driven by a brush dc motor [73,74]:

$$\begin{cases} \bar{M}\ddot{q} + \bar{N}\sin(q) + \bar{B}\dot{q} = I + \Delta I \\ L\dot{I} = -RI - K_B\dot{q} + V \\ y = q \end{cases} \tag{85}$$

where $q, \dot{q}$ and $\ddot{q}$ are angular position, angular velocity and angular acceleration, I is motor armature current, ΔI is current disturbance, V is input control voltage and the physical meaning of other parameters can be found in [73]. Let $x_1 = q, x_2 = \dot{q}, x_3 = I, u = V$ and the system (85) can be written as

$$\begin{cases} \dot{x_1} = x_2 \\ \dot{x_2} = -\frac{\bar{N}}{\bar{M}}sin(x_1) - \frac{\bar{B}}{\bar{M}}x_2 + \frac{1}{\bar{M}}x_3 + \frac{\Delta I}{\bar{M}} \\ \dot{x_3} = -\frac{R}{L}x_3 - \frac{K_B}{L}x_2 + \frac{u}{L} \\ y = x_1 \end{cases} \tag{86}$$

The parameters in system (86) can be selected as $\bar{N} = 10$, $\bar{B} = 1$, $\bar{M} = 1$, $L = 0.05$, $K_B = 0.5$, $R = 0.5$ and the current disturbance is assumed to be $\Delta I =$

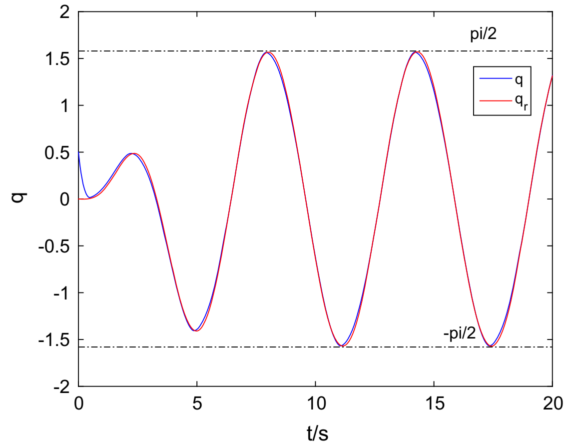

Fig. 7 Time response of system output q and its reference q_r

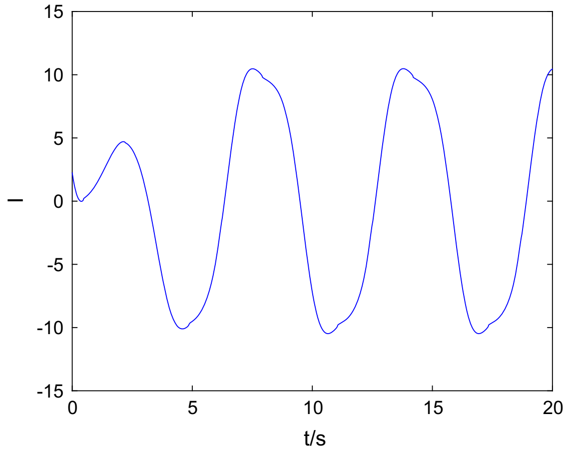

Fig. 8 Time response of the motor armature current I

$0.1x_1 \sin(x_2x_3)$. Since the disturbance contains all the state variables, system (86) is a nonstrict-feedback system. The reference output is $y_r = \pi/2 \sin(t)(1 - e^{-0.1t^2})$ and the output constraint is selected as $|y| < \pi/2$. In this example, $\underline{g}_1 = \bar{g}_1 = \underline{g}_2 = \bar{g}_2 = 1$, $\underline{g}_3 = \bar{g}_3 = 20$. Dead zone and input saturation parameters are selected to be the same as Example 1. The design parameters for virtual control, parameter adaptive law and first-order sliding mode differentiator are chosen as $k_1 = k_2 = k_3 = 5$, $\eta_1 = \eta_2 = \eta_3 = 3$, $\Lambda_1 = \Lambda_2 = \Lambda_3 = 2.5$, $\kappa_1 = \kappa_2 = 5$, $\Gamma_1 = \Gamma_2 = \Gamma_3 = 0.8$, $\sigma_1 = \sigma_2 = \sigma_3 = 10$, $\gamma_1 = \gamma_2 = \gamma_3 = 0.1$, $\Pi_1 = \Pi_2 = 10$, $\mu_1 = \mu_2 = 4.5$, $k = 10$, $\xi = 5$, $\tau = 0.1$, $\lambda_0 = 1.5$, $\lambda_1 = 1.1$. The results are shown in Figs. 7, 8 and 9. Figures 7 and 8 show the time response of states q and I, and Fig. 9 depicts the curve

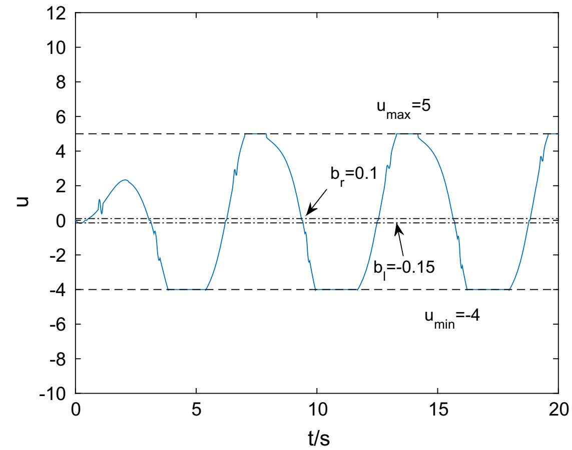

Fig. 9 Curve of control voltage u

of control voltage u. It can be seen from these figures that the system output track the trajectory of reference output within finite time while the violation of output constraint is avoided and desired control performance is obtained.

6 Conclusion

In this paper, an adaptive neural network dynamic surface control is presented for a class of nonstrict-feedback uncertain nonlinear systems subjected to input saturation, dead zone and output constraint. By designing anti-windup compensator, the input saturation problem is solved. Tan-type Barrier Lyapunov function is introduced to prevent output constraint violation. Furthermore, using adaptive backstepping technique, a series of novel stabilizing virtual control functions are derived. In order to overcome the explosion of complexity, first-order sliding mode differentiator is employed to obtain the derivative of virtual control. Using dead zone inverse method, the real control input is obtained. With the aid of finite time stability theory, it is proved that the proposed control scheme can drive the output tracking error into a small neighbor of the origin within finite time and keep all the closed-loop signals bounded. Simulation results demonstrate the effectiveness of the proposed control scheme. In the future, there are many researches to be done, for example, how to develop a control scheme to take hysteresis effects into account, how to extend the proposed control scheme to time delay system, switched system, multi-input and multi-output system and stochastic system, how to extend the proposed control scheme to address fault-tolerant control problem, how to utilize fuzzy system to approximate the studied system and design controller and observer with the aid of the existing results [75–78], how to extend the proposed control scheme to study consensus problem of nonlinear multi-agent system using the idea of the existing result [79]. In addition, the control of bifurcation has received great attention and many control schemes have been proposed, such as PD control [80], state feedback control [81] and sliding mode control [82]. Recently, adaptive neural network backstepping control scheme [83] was presented to control bifurcation. Therefore, the extension of the proposed control scheme to bifurcation control is another future research direction.

Acknowledgements This research did not receive any specific grant from funding agencies in the public, commercial, or not-for-profit sectors.

Compliance with ethical standards

Conflict of interest The authors declare that they have no conflict of interest concerning the publication of this manuscript.

References

1. Park, J., Sandberg, I.W.: Universal approximation using radial-basis-function networks. Neural Comput. **3**, 246–257 (1991)
2. Yoo, S.J., Park, J.B., Choi, Y.H.: Adaptive output feedback control of flexible-joint robots using neural networks: dynamic surface design approach. IEEE Trans. Neural Netw. **19**, 1712–1726 (2008)
3. El-Sousy, F.F.M.: Intelligent optimal recurrent wavelet Elman neural network control system for permanent-magnet synchronous motor servo drive. IEEE Trans. Indus. Inform. **9**, 1986–2003 (2013)
4. Chu, Z.Z., Zhu, D.Q., Yang, S.X.: Observer-based adaptive neural network trajectory tracking control for remotely operated vehicle. IEEE Trans. Neural Netw. Learn. Syst. **28**, 1633–1645 (2017)
5. Hu, S.L., Yue, D., Xie, X.P., Ma, Y., Yin, X.X.: Stabilization of neural-network-based control systems via event-triggered control with nonperiodic sampled data. IEEE Trans. Neural Netw. Learn. Syst. **29**, 573–585 (2018)
6. Zhang, Y.Y., Chen, S.Y., Li, S., Zhang, Z.J.: Adaptive projection neural network for kinematic control of redundant manipulators with unknown physical parameters. IEEE Trans. Ind. Electron. **65**, 4909–4920 (2018)
7. Yang, C.G., Wang, X.J., Li, Z.J., Li, Y.N., Su, C.Y.: Teleoperation control based on combination of wave variable and neural networks. IEEE Trans. Syst. Man Cybern. Syst. **47**, 2125–2136 (2017)
8. Wang, H.Q., Shi, P., Li, H.Y., Zhou, Q.: Adaptive neural tracking control for a class of nonlinear systems with dynamic uncertainties. IEEE Trans. Cybern. **47**, 3075–3087 (2017)
9. Sun, H.B., Guo, L.: Neural network-based DOBC for a class of nonlinear systems with unmatched disturbances. IEEE Trans. Neural Netw. Learn. Syst. **28**, 482–489 (2017)
10. Ge, S.S., Wang, C.: Adaptive neural control of uncertain MIMO nonlinear systems. IEEE Trans. Neural Netw. **15**, 674–692 (2004)
11. Zhou, Q., Shi, P., Xu, S.Y., Li, H.Y.: Observer-based adaptive neural network control for nonlinear stochastic systems with time delay. IEEE Trans. Neural Netw. Learn. Syst. **24**, 71–80 (2013)
12. Wang, M., Liu, X.P., Shi, P.: Adaptive neural control of pure-feedback nonlinear time-delay systems via dynamic surface technique. IEEE Trans. Syst. Man Cybern. B Cybern. **41**, 1681–1692 (2011)
13. Shafiei, S.E., Soltanpour, M.R.: Robust neural network control of electrically driven robot manipulator using backstepping approach. Int. J. Adv. Robot. Syst. **6**, 285–292 (2009)
14. Wai, R.-J., Chang, H.-H.: Backstepping wavelet neural network control for indirect field-oriented induction motor drive. IEEE Trans. Neural Netw. **15**, 367–382 (2004)
15. Niu B, Ahn CK, Li H, Liu M.: Adaptive control for stochastic switched non-lower triangular nonlinear systems and its application to one-link manipulator. IEEE Trans. Syst. Man Cybern. Syst. https://doi.org/10.1109/TSMC.2017.2685638 (2017)
16. Wang, D., Huang, J.: Neural network-based adaptive dynamic surface control for a class of uncertain nonlinear systems in strict-feedback form. IEEE Trans. Neural Netw. **16**, 195–202 (2005)
17. Yang, Y., Yue, D., Xie, X.P.: Adaptive fault-tolerant tracking control of a class of uncertain nonlinear systems with actuator faults. In: Proceedings of the 35th Chinese Control Conference, Chengdu, China, pp. 556–561 (2016)
18. Wang, D.: Neural network-based adaptive dynamic surface control of uncertain nonlinear pure-feedback systems. Int. J. Robust Nonlinear Control **21**, 527–541 (2011)
19. Chen, W.S., Jiao, L.C., Du, Z.B.: Output-feedback adaptive dynamic surface control of stochastic non-linear systems using neural network. IET Control Theory Appl. **4**, 3012–3021 (2010)
20. Peng, Z.H., Wang, D., Chen, Z.Y., Hu, X.J., Lan, W.Y.: Adaptive dynamic surface control for formations of autonomous surface vehicles with uncertain dynamics. IEEE Trans. Control Syst. Technol. **21**, 513–520 (2013)
21. Xu, B., Zhang, Q., Pan, Y.P.: Neural network based dynamic surface control of hypersonic flight dynamics using small-gain theorem. Neurocomputing **173**, 690–699 (2016)
22. Xu, B., Yang, C.G., Pan, Y.P.: Global neural dynamic surface tracking control of strict-feedback systems with application to hypersonic flight vehicle. IEEE Trans. Neural Netw. Learn. Syst. **26**, 2563–2575 (2015)
23. Zong, Q., Wang, F., Tian, B.L., Su, R.: Robust adaptive dynamic surface control design for a flexible air-breathing hypersonic vehicle with input constraints and uncertainty. Nonlinear Dyn. **78**, 289–315 (2014)
24. Mehraeen, S., Jagannathan, S., Crow, M.L.: Power system stabilization using adaptive neural network-based dynamic

surface control. IEEE Trans. Power Syst. **26**, 669–680 (2011)
25. Yu, J.P., Shi, P., Dong, W.J., Chen, B., Lin, C.: Neural network-based adaptive dynamic surface control for permanent magnet synchronous motors. IEEE Trans. Neural Netw. Learn. Syst. **26**, 640–645 (2015)
26. Kogiso, K., Hirata, K.: Reference governor for constrained systems with time-varying references. Robot. Auton. Syst. **57**, 289–295 (2009)
27. Jin, X., Wang, Z.W., Kwong, R.H.S.: Convex optimization-based iterative learning control for iteration-varying systems under output constraints. In: Proceedings of the 11th IEEE International Conference on Control and Automation (IEEE ICCA), Taichung, ITaiwan, pp. 1444–1448 (2014)
28. Niu, B., Zhao, X.D., Yang, X.B., Fan, X.D.: Tracking and H_∞ control of constrained nonlinear switched systems in strict feedback form. Nonlinear Dyn. **80**, 87–100 (2015)
29. Meng, W.C., Yang, Q.M., Sun, Y.X.: Adaptive neural control of nonlinear MIMO systems with time-varying output constraints. IEEE Trans. Neural Netw. Learn. Syst. **26**, 1074–1085 (2015)
30. Chang, W.M., Tong, S.C.: Adaptive fuzzy tracking control design for permanent magnet synchronous motors with output constraint. Nonlinear Dyn. **87**, 291–302 (2017)
31. Zhang, S., Dong, Y.T., Ouyang, Y.C., Zhao, Y., Peng, K.X.: Adaptive neural control for robotic manipulators with output constraints and uncertainties. IEEE Trans. Neural Netw. Learn. Syst. https://doi.org/10.1109/TNNLS.2018.2803827 (2018)
32. Jin, X.: Adaptive finite-time fault-tolerant tracking control for a class of MIMO nonlinear systems with output constraints. Int. J. Robust Nonlinear Control **27**, 722–741 (2017)
33. Chen, Z.T., Li, Z.J., Chen, C.L.P.: Adaptive neural control of uncertain MIMO nonlinear systems with state and input constraints. IEEE Trans. Neural Netw. Learn. Syst. **28**, 1318–1330 (2017)
34. He, W., Li, Z.J., Chen, C.L.P.: A survey of human-centered intelligent robots: issues and challenges. IEEE/CAA J. Autom. Sin. **4**, 602–609 (2017)
35. Tee, K.P., Ren, B.B., Ge, S.S.: Control of nonlinear systems with time-varying output constraints. Automatica **47**, 2511–2516 (2011)
36. He, W., Huang, H.F., Chen, Y., Xie, W.Z., Feng, F.S., Kang, Y.M., Sun, C.Y.: Development of an autonomous flapping-wing aerial vehicle. Sci. China-Inf. Sci. **60**, 063201 (2017)
37. Liu, Y.-J., Lu, S.M., Tong, S.C.: Neural network controller design for an uncertain robot with time-varying output constraint. IEEE Trans. Syst. Man Cybern. Syst. **47**, 2060–2068 (2017)
38. Ibrir, S., Xie, W.F., Su, C.-Y.: Adaptive tracking of nonlinear systems with non-symmetric dead-zone input. Automatica **43**, 522–530 (2007)
39. Ma, H.-J., Yang, G.-H.: Adaptive output control of uncertain nonlinear systems with non-symmetric dead-zone input. Automatica **46**, 413–420 (2010)
40. Su, C.-Y., Stepanenko, Y., Svoboda, T.P.L.: Robust adaptive control of a class of nonlinear systems with unknown backlash-like hysteresis. IEEE Trans. Autom. Control **45**, 2427–2432 (2000)
41. Wang, X.S., Su, C.Y., Hong, H.: Robust adaptive control of a class of linear systems with unknown dead-zone. Automatica **40**, 407–413 (2004)
42. Liu, S.Y., Liu, Y.C., Wang, N.: Robust adaptive self-organizing neuro-fuzzy tracking control of UUV with system uncertainties and unknown dead-zone nonlinearity. Nonlinear Dyn. **89**, 1397–1414 (2017)
43. He, W., He, X.Y., Sun, C.Y.: Vibration control of an industrial moving strip in the presence of input deadzone. IEEE Trans. Ind. Electron. **64**, 4680–4689 (2017)
44. Zhou, J., Wen, C., Zhang, Y.: Adaptive output control of nonlinear systems with uncertain dead-zone nonlinearity. IEEE Trans. Autom. Control **51**, 504–511 (2006)
45. Tong, S.C., Li, Y.M.: Adaptive fuzzy output feedback tracking backstepping control of strict-feedback nonlinear systems with unknown dead zones. IEEE Trans. Fuzzy Syst. **20**, 168–180 (2012)
46. Selmis, R.R., Lewis, F.L.: Dead-zone compensation in motion control systems using neural networks. IEEE Trans. Autom. Control **45**, 602–613 (2000)
47. Lewis, F.L., Tim, W.K., Wang, L.-Z., Li, Z.X.: Deadzone compensation in motion control systems using adaptive fuzzy logic control. IEEE Trans. Control Syst. Technol. **7**, 731–742 (1999)
48. Chen, M., Ge, S.S., Ren, B.B.: Adaptive tracking control of uncertain MIMO nonlinear systems with input constraints. Automatica **47**, 452–465 (2011)
49. Zhang, S., Dong, Y.T., Ouyang, Y.C., Yin, Z., Peng, K.X.: Adaptive neural control for robotic manipulators with output constraints and uncertainties. IEEE Trans. Neural Netw. Learn. Syst. https://doi.org/10.1109/TNNLS.2018.2803827 (2018)
50. Li, Y.M., Tong, S.C., Li, T.S.: Hybrid fuzzy adaptive output feedback control design for uncertain MIMO nonlinear systems with time-varying delays and input saturation. IEEE Trans. Fuzzy Syst. **24**, 841–853 (2016)
51. Meng, T.T., He, W.: Iterative learning control of a robotic arm experiment platform with input constraint. IEEE Trans. Ind. Electron. **65**, 664–672 (2018)
52. Li, Y.M., Tong, S.C., Li, T.S.: Composite adaptive fuzzy output feedback control design for uncertain nonlinear strict-feedback systems with input saturation. IEEE Trans. Cybern. **45**, 2299–2308 (2015)
53. Chen, M., Tao, G., Jiang, B.: Dynamic surface control using neural networks for a class of uncertain nonlinear systems with input saturation. IEEE Trans. Neural Netw. Learn. Syst. **26**, 2086–2097 (2015)
54. Shen, Q.K., Shi, P., Shi, Y., Zhang, J.H.: Adaptive output consensus with saturation and dead-zone and its application. IEEE Trans. Ind. Electron. **64**, 5025–5034 (2017)
55. Cui, R.X., Zhang, X., Cui, D.: Adaptive sliding-mode attitude control for autonomous underwater vehicles with input nonlinearities. Ocean Eng. **123**, 45–54 (2016)
56. Li, Y.M., Tong, S.C.: Command-filtered-based fuzzy adaptive control design for MIMO-switched nonstrict-feedback nonlinear systems. IEEE Trans. Fuzzy Syst. **25**, 668–681 (2017)
57. Tong, S.C., Li, Y.M., Sui, S.: Adaptive fuzzy output feedback control for switched nonstrict-feedback nonlinear systems with input nonlinearities. IEEE Trans. Fuzzy Syst. **24**, 1426–1440 (2016)

58. Wang, L.J., Li, H.Y., Zhou, Q., Lu, R.Q.: Adaptive fuzzy control for nonstrict feedback systems with unmodeled dynamics and fuzzy dead zone via output feedback. IEEE Trans. Cybern. **47**, 2400–2412 (2017)
59. Wu, J., Su, B.Y., Li, J., Zhang, X., Li, X.B., Chen, W.S.: Adaptive fuzzy control for full states constrained systems with nonstrict-feedback form and unknown nonlinear dead zone. Inf. Sci. **376**, 233–247 (2017)
60. Zhou, Q., Wang, L.J., Wu, C.W., Li, H.Y., H.P, Du: Adaptive fuzzy control for nonstrict-feedback systems with input saturation and output constraint. IEEE Trans. Syst. Man Cybern. Syst. **47**, 1–12 (2017)
61. Chen, B., Liu, X.P., Ge, S.S., Lin, C.: Adaptive fuzzy control of a class of nonlinear systems by fuzzy approximation approach. IEEE Trans. Fuzzy Syst. **20**, 1012–1021 (2012)
62. Chen, B., Lin, C., Liu, X.P., Liu, K.F.: Adaptive fuzzy tracking control for a class of MIMO nonlinear systems in nonstrict-feedback form. IEEE Trans. Cybern. **45**, 2744–2755 (2015)
63. Liu, Z.L., Chen, B., Lin, C.: Adaptive neural backstepping for a class of switched nonlinear system without strict-feedback form. IEEE Trans. Syst., Man, Cybern. Syst. **47**, 1315–1320 (2017)
64. Cai, M.J., Xiang, Z.R.: Adaptive practical finite-time stabilization for uncertain nonstrict feedback nonlinear systems with input nonlinearity. IEEE Trans. Syst. Man Cybern. Syst. **47**, 1668–1678 (2017)
65. Shi, X.C., Xu, S.Y., Chen, W.M., Zhang, Z.Q.: Adaptive neural control of switched nonstrict-feedback nonlinear systems with multiple time-varying delays. J. Frankl. Inst. Eng. Appl. Math. **354**, 8180–8199 (2017)
66. Wang, C., Lin, Y.: Decentralized adaptive tracking control for a class of interconnected nonlinear time-varying systems. Automatica **54**, 16–24 (2015)
67. Hardy, G., Littlewood, J., Polya, G.: Inequalities. Cambridge University Press, London (1951)
68. Zuo, Z.Y., Tie, L.: A new class of finite-time nonlinear consensus protocols for multi-agent systems. Int. J. Control **87**, 363–370 (2014)
69. Yu, S.H., Yu, X.H., Shirinzadeh, B., Man, Z.H.: Continuous finite-time control for robotic manipulators with terminal sliding mode. Automatica **41**, 1957–1964 (2005)
70. Polycarpou, M.M., Ioannou, P.A.: A robust adaptive nonlinear control design. Automatica **32**, 423–427 (1996)
71. Levant, A.: Robust exact differentiation via sliding mode technique. Automatica **34**, 379–384(1998)
72. Chen, M., Ge, S.S.: Adaptive neural output feedback control of uncertain nonlinear systems with unknown hysteresis using disturbance observer. IEEE Trans. Ind. Electron. **62**, 7706–7716 (2015)
73. Carroll, J.J., Dawson, D.M.: Integrator backstepping techniques for the tracking control of permanent magnet brush DC motors. IEEE Trans. Ind. Appl. **31**, 248–255 (1995)
74. Li, Q.N., Yang, R.N., Liu, Z.C.: Adaptive tracking control for a class of nonlinear non-strict-feedback systems. Nonlinear Dyn. **88**, 1537–1550 (2017)
75. Xie, X.P., Yue, D., Zhang, H.G., Xue, Y.S.: Control synthesis of discrete-time T-S fuzzy systems via a multi-instant homogenous polynomial approach. IEEE Trans. Cybern. **46**, 630–640 (2016)
76. Xie, X.P., Yang, D.S., Ma, H.J.: Observer design of discrete-time T-S fuzzy systems via multi-instant homogenous matrix polynomials. IEEE Trans. Fuzzy Syst. **22**, 1714–1719 (2014)
77. Xie, X.P., Yue, D., Ma, T.D., Zhu, X.L.: Further studies on control synthesis of discrete-time T-S fuzzy systems via augmented multi-indexed matrix approach. IEEE Trans. Cybern. **44**, 2784–2791 (2014)
78. Zhou, Q., Li, H.Y., Wu, C.W., Wang, L.J., Ahn, C.K.: Adaptive fuzzy control of nonlinear systems with unmodeled dynamics and input saturation using small-gain approach. IEEE Trans. Syst. Man Cybern. Syst. **47**, 1979–1989 (2017)
79. Agha, R., Rehan, M., Ahn, C.K., Mustafa, G., Ahmad, S.: Adaptive distributed consensus control of one-sided Lipschitz nonlinear multi-agents. IEEE Trans. Syst. Man Cybern. Syst. https://doi.org/10.1109/TSMC.2017.2764521 (2017)
80. Tang, Y.H., Xiao, M., Jiang, G.P., Lin, J.X., Cao, J.D., Zheng, W.X.: Fractional-order PD control at Hopf bifurcations in a fractional-order congestion control system. Nonlinear Dyn. **90**, 2185–2198 (2017)
81. Xiao, M., Jiang, G.P., Zhao, L.D.: State feedback control at Hopf bifurcation in an exponential RED algorithm model. Nonlinear Dyn. **76**, 1469–1484 (2014)
82. Moradi, H., Abbasi, M.H., Moradian, H.: Improving the performance of a nonlinear boiler-turbine unit via bifurcation control of external disturbances: a comparison between sliding mode and feedback linearization control approaches. Nonlinear Dyn. **85**, 229–243 (2016)
83. Luo, S.H., Song, Y.D.: Chaos analysis-based adaptive backstepping control of the microelectromechanical resonators with constrained output and uncertain time delay. IEEE Trans. Ind. Electron. **63**, 6217–6225 (2016)